Development/Plasticity/Repair

Nurr1 Is Required for Maintenance of Maturing and Adult Midbrain Dopamine Neurons

Banafsheh Kadkhodaei,[1] Takehito Ito,[2] Eliza Joodmardi,[1] Bengt Mattsson,[3] Claude Rouillard,[1] Manolo Carta,[3] Shin-Ichi Muramatsu,[4] Chiho Sumi-Ichinose,[5] Takahide Nomura,[5] Daniel Metzger,[6] Pierre Chambon,[6] Eva Lindqvist,[7] Nils-Göran Larsson,[8,10] Lars Olson,[7] Anders Björklund,[3] Hiroshi Ichinose,[2] and Thomas Perlmann[1,9]

[1]Ludwig Institute for Cancer Research, Stockholm Branch, SE-171 77 Stockholm, Sweden, [2]Graduate School of Bioscience and Biotechnology, Tokyo Institute of Technology, Yokohama 226-8501, Japan, [3]Wallenberg Neuroscience Center, Lund University, SE-221 84 Lund, Sweden, [4]Department of Neurology, Jichi Medical University, Tochigi 329-0498, Japan, [5]Department of Pharmacology, Fujita Health University School of Medicine, Toyoake, Aichi 470-1192, Japan, [6]Department of Functional Genomics Institut de Génétique et Biologie Moléculaire et Cellulaire, 67404 Illkirch, France, Departments of [7]Neuroscience, [8]Laboratory Medicine, and [9]Cell and Molecular Biology, Karolinska Institutet, SE-171 77 Stockholm, Sweden, and [10]Max Planck Institute for Biology of Ageing, D-50931 Cologne, Germany

Transcription factors involved in the specification and differentiation of neurons often continue to be expressed in the adult brain, but remarkably little is known about their late functions. Nurr1, one such transcription factor, is essential for early differentiation of midbrain dopamine (mDA) neurons but continues to be expressed into adulthood. In Parkinson's disease, Nurr1 expression is diminished and mutations in the *Nurr1* gene have been identified in rare cases of disease; however, the significance of these observations remains unclear. Here, a mouse strain for conditional targeting of the *Nurr1* gene was generated, and *Nurr1* was ablated either at late stages of mDA neuron development by crossing with mice carrying Cre under control of the dopamine transporter locus or in the adult brain by transduction of adeno-associated virus Cre-encoding vectors. *Nurr1* deficiency in maturing mDA neurons resulted in rapid loss of striatal DA, loss of mDA neuron markers, and neuron degeneration. In contrast, a more slowly progressing loss of striatal DA and mDA neuron markers was observed after ablation in the adult brain. As in Parkinson's disease, neurons of the substantia nigra compacta were more vulnerable than cells in the ventral tegmental area when *Nurr1* was ablated at late embryogenesis. The results show that developmental pathways play key roles for the maintenance of terminally differentiated neurons and suggest that disrupted function of Nurr1 and other developmental transcription factors may contribute to neurodegenerative disease.

Introduction

Adaptation to a changing environment requires plasticity in the adult CNS. However, to ensure that neurons are properly maintained, such plasticity must be balanced against mechanisms that counteract phenotypic instability. Studies of how neurons develop may help to unravel functions important for the stability of nerve cells as factors promoting their differentiation may also contribute to their maintenance. Indeed, many transcription factors identified for their critical roles during neuronal development continue to be expressed in the postnatal nervous system, raising the possibility that they contribute to the integrity of already differentiated neurons (Hendricks et al., 1999; Vult von Steyern et al., 1999; Kang et al., 2007; Alavian et al., 2008). However, the consequences of adult gene ablation of any of these factors have not yet been reported, and very little is known of their functions in differentiated neurons.

From a clinical perspective, it is of particular interest to identify factors that maintain stability of neurons that are affected in neurodegenerative disorders as loss of phenotype would likely cause or contribute to disease. Parkinson's disease (PD) is characterized by progressive pathology of midbrain dopamine (mDA) neurons of substantia nigra pars compacta (SNc) and the ventral tegmental area (VTA), typically involving deposition of α-synuclein-rich cytoplasmic protein aggregates termed Lewy bodies. During development, early signaling events induce transcription factors that control the specification and differentiation of mDA neurons (Smidt and Burbach, 2007). Several of these factors, including Nurr1, Lmx1a, Lmx1b, Pitx3, FoxA2, and En1/2, continue to be expressed in the postnatal and adult brain (Zetterström et al., 1996; Smidt et al., 1997, 2000; Albéri et al., 2004; Simon et al., 2004; Kittappa et al., 2007). Nurr1, belonging to a family of ligand-independent nuclear receptors (Wang et al., 2003; Perlmann and Wallén-Mackenzie, 2004), becomes expressed in developing mDA neurons that have just exited the cell cycle and is essential for mDA neuron development because mDA neurons of both the SNc and VTA fail to express dopaminergic markers and newborn *Nurr1*-null mice lack mDA neuron cell bodies and their striatal projections (Zetterström et al., 1997; Castillo et al., 1998; Saucedo-Cardenas et al., 1998). How Nurr1 regulates target genes in mDA neuron development remains essentially unknown but may involve a functional interaction with the homeobox transcription factor Pitx3 (Jacobs et al., 2009).

Determining the role of Nurr1 also in the adult brain is of particular importance because previous studies suggested an association of this protein with PD pathology. Nurr1 expression is diminished in neurons with α-synuclein inclusions in postmortem PD brain tissue, and *Nurr1* mutations and polymorphisms have been identified in rare cases of PD (Xu et al., 2002; Le et al., 2003; Zheng et al., 2003; Grimes et al., 2006). However, the significance of genetic lesions remain unclear (Wellenbrock et al., 2003; Hering et al., 2004; Tan et al., 2004). These observations emphasize the importance of elucidating the role of Nurr1 in more mature mDA neurons by analyzing the consequences of conditional *Nurr1* gene ablation in mice.

Materials and Methods

Conditional Nurr1 gene-targeted mice. Mouse 129SV genomic library constructed in bacterial artificial chromosome (BAC) was screened by PCR. A BAC clone containing the entire Nurr1 gene was selected, and a BamHI–MunI fragment containing exon 1 to exon 5 was recloned into a pBluescript II vector. A floxed neomycin cassette was inserted into an internal EcoRI site located in intron 3, and a synthetic loxP sequence was inserted at SalI site located in intron 2. Mouse embryonic stem (ES) cells were electroporated with the targeting vector, and the homologously recombinated clones were screened by PCR and Southern blot analysis. ES clones with three loxP sites were selected, and a plasmid expressing Cre DNA recombinase was transiently transfected into the cells. ES cells with two loxP sites without a neomycin cassette were selected by PCR and used for production of chimeric mice.

Animals. Mice were kept in rooms with controlled 12 h light/dark cycles, temperature, and humidity, with food and water provided *ad libitum*. All animal experiments were performed with permission from the local animal ethics committee. The generation of dopamine transporter (*DAT*)–*Cre* mutant mice has been described previously (Ekstrand et al., 2007). Mice were mated during the night, and the females were checked for vaginal plugs in the morning [day of vaginal plug considered as embryonic day 0.5 (E0.5)].

L-3,4-Dihydroxyphenylalanine treatment. Methyl L-3,4-dihydroxyphenylalanine (L-DOPA) hydrochloride and the peripheral DOPA decarboxylase inhibitor benserazide-HCl (Sigma-Aldrich) were dissolved in Ringer's solution immediately before use. L-DOPA was intraperitoneally given every second day at the dose of 2.5 mg/kg combined with 0.625 mg/kg benserazide. Chronic treatment with L-DOPA/benserazide was administered for 50 d, starting at postnatal day 15 (P15). During this period, the mice were carefully observed and weight was measured regularly. Reported hyperactivity was observed in $cNurr1^{DATCre}$ mice when given a single higher dose of L-DOPA (25 mg/kg L-DOPA, 6.25 mg/kg benserazide).

Histological analyses. At embryo stages, embryos were fixed for 2–24 h in 4% phosphate-buffered paraformaldehyde (PFA), cryopreserved in 30% sucrose before being embedded in OCI (Sakura Finetek), and cryosectioned at a thickness of 10–20 μm onto slides (SuperFrostPlus; Menzel Gläser). For the isolation of brains for immunolabeling at P15 and onward, animals were anesthetized with Avertin (tribromoethanol; 0.5 mg/g) and perfused through the left ventricle with body-temperature PBS, followed by ice-cold 4% PFA. The brains were dissected and post-fixed overnight in 4% paraformaldehyde and subsequently cryoprotected for 24–48 h in 30% sucrose at 4°C. The brains were serially sectioned on a cryostat or sliding microtome at 10–30 μm. Littermates were used in an all comparative experiments.

For immunohistochemistry, sections were preincubated for 1 h in blocking solution containing either 10% normal goat sera or 5–10% bovine serum albumin, 0.25% Triton X-100, and 0.01% Na-azide in PBS. Primary antibodies diluted in blocking solution were applied overnight at 4°C. After rinses with PBS, biotinylated- or fluorophore-conjugated secondary antibodies diluted in PBS were applied for 1 h at room temperature. Biotinylated secondary antibodies were followed by incubation with streptavidin–horseradish peroxidase complex (ABC elite kit, Vectastain) for 1 h and subsequent exposure to diaminobenzidine (DAB kit; Vector Laboratories). Primary antibodies and dilution factors were as follows: rabbit anti-Nurr1 (1:100; M196; Santa Cruz Biotechnology), anti-Nurr1 (1:250; E20; Santa Cruz Biotechnology), rabbit anti-tyrosine hydroxylase (TH) (1:500; Pel-Freeze), rat anti-DAT (1:2000; Millipore Bioscience Research Reagents), mouse anti-TH (1:200; Millipore Bioscience Research Reagents), rabbit anti-vesicular monoamine transporter (VMAT) (1:500; Millipore Bioscience Research Reagents), rabbit anti-L-DOPA decarboxylase (AADC) (1:500; Millipore Bioscience Research Reagents), rabbit anti-Cre (1:10,000; Covance Research Products), guinea pig anti-Lmx1b (1:1000) (Andersson et al., 2006), and rabbit anti-Pitx3 (Smidt et al., 2004). In some cases (anti-AADC, anti-VMAT, and anti-Nurr1), the blocking steps were performed after antigen retrieval (Dako). Finally, expression was detected by secondary antibodies from Jackson ImmunoResearch. Section images were collected by confocal microscopy (Leica DMIRE2) and bright-field microscopy (Eclipse E1000K; Nikon). Cell counting was performed by counting all SNc DA neurons detected by immunohistochemistry (DAB) in a total of three sections per animal (every 12th tissue section) within the ventral midbrain of animals taken at 4 months after vector injection in both wild-type wt^{AAVCre} and $cNurr1^{AAVCre}$ animals. The mean of counted cells per animal was established from both the injected and non-injected sides in each animal, and the relative decrease was calculated as a percentage as described in Results.

AAV–Cre injections. Two and a half- to 5-month-old animals received one unilateral stereotaxic injection in the right striatum using a 10 μl Hamilton microsyringe fitted with a glass pipette tip. The animals were anesthetized with isoflurane, 1 μl was injected during 5 min, and the cannula was left in place for an additional 2 min before being slowly retracted. The anteroposterior and mediolateral coordinates from bregma were −2.8 and −1.1 mm, respectively, and the dorsoventral coordinates from the dura were −4.3 mm. Animals were killed 0.5, 1.5, and 4 months after injection, and the brains were isolated.

Measurement of tissue content for dopamine, serotonin, and their metabolites. In supplemental Tables 1–3 (available at www.jneurosci.org as supplemental material), tissues were collected from P1, P7, P14, and adult (P48) wt^{DATCre} and $cNurr1^{DATCre}$ mice. One- to 14-d-old mice were killed by decapitation, and P48 mice were killed by cervical dislocation. Brains were rapidly removed, chilled in saline (4°C), dissected, frozen on dry ice, and stored at −80°C until use. To process tissues for HPLC and electrochemical detection of monoamines and metabolites, samples were homogenized by sonication in 5 vol or in 30 μl of 0.1 M perchloric acid, followed by centrifugation. Endogenous levels of noradrenaline, DA, 3,4-dihydroxyphenylacetic acid, homovanillic acid (HVA), serotonin (5-HT), and 5-hydroxyindoleacetic acid were determined in the supernatants. A reverse column (BAS, C-18, 100.0 × 3.2 mm, 3 μm particle diameter) was used for separation. The mobile phase consisted of 0.05 M sodium phosphate/0.03 M citric acid buffer containing 0.1 mM EDTA and was adjusted with various amounts of methanol and sodium-L-octane sulfonic acid. The flow rate was 0.3 ml/min. Monoamines and metabolites were detected using a glassy-carbon electrode detector, which as set at +0.7 V versus an Ag/AgCl reference electrode. Resultant peaks were measured and compared with repeated control samples containing fixed mixed amounts of compounds of interest.

In supplemental Table 4 (available at www.jneurosci.org as supplemental material), all animals were killed, and striata and cortex were rapidly dissected out, frozen on dry ice, and stored at −80°C. To determine monoamines, tissue was homogenized in 0.1 M perchloric acid and centrifuged at 10,000 rpm for 10 min before filtering though minispin filters for an additional 3 min at 10,000 rpm. The tissue extract were then analyzed by HPLC as described previously (Carta et al., 2007) with minor

Received Aug. 11, 2009; revised Oct. 17, 2009; accepted Oct. 28, 2009.

This work was supported by grants from the Michael J. Fox Foundation (T.P., A.B., L.O.), Vetenskapsrådet via Linné Center DBRM (T.P.), Grants-in-Aid for Human Frontier Science Program (P.C., D.M., H.I.), Grants-in-Aid for Scientific Research from the Ministry of Education, Culture, Sports, Science, and Technology of Japan, the Ministry of Health, Labor, and Welfare of Japan, and the Japan Science and Technology Agency, Core Research for Evolutional Science and Technology (S.-I.M., H.I.), Vetenskapsrådet (L.O.), Swedish Brain Power (L.O.), Swedish Brain Foundation (L.O.), and the Swedish Parkinson Foundatin (L.O.). We are grateful to Johan Ericson and members of the Perlmann and Ericson laboratories for valuable discussions. We thank Andrée Dierich and Jean-Marc Bornert for their help in mouse mutagenesis, Noriko Ihira for help in construction of the targeting vector and screening of ES clones, Björn Anzelius and Naomi Takino for their help with AAV vectors, Ulla Jarl for help with histology, and Marie-Louise Ajun for advice on mice handling.

Correspondence should be addressed to either of the following: Thomas Perlmann, Department of Cell and Molecular Biology, Karolinska Institutet, SE-171 77 Stockholm, Sweden, E-mail: thomas.perlmann@licr.ki.se; or Hiroshi Ichinose, Graduate School of Bioscience and Biotechnology, Tokyo Institute of Technology, Yokohama 226-8501, Japan, E-mail: hichinos@bio.titech.ac.jp.

DOI:10.1523/JNEUROSCI.3910-09.2009

 0270-6474/09/2915923-10$15.00/0

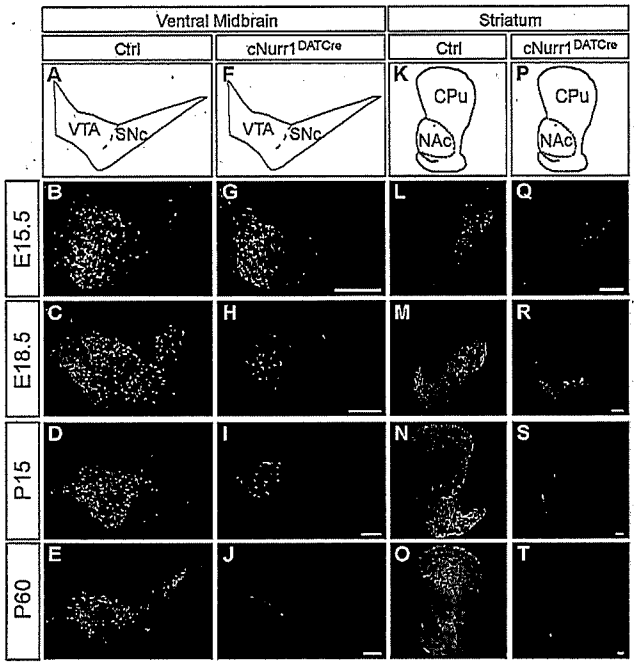

Figure 1. TH is progressively lost in both the ventral midbrain and striatum of *cNurr1*^{DATCre} mice. *A–T*, Confocal microscopy showing TH immunohistochemistry in control (ctrl) and *cNurr1*^{DATCre} mice as indicated. *A–J*, Sections were analyzed at the levels of ventral midbrain (as indicated in *A* and *F*) and in the striatum (as indicated in *K* and *P*). TH immunofluorescence was analyzed at both embryonal and postnatal stages as indicated. Results demonstrate a progressive loss of TH immunoreactivity in the ventral midbrain. Note that TH immunoreactivity was more drastically downregulated at more lateral regions compared with the prospective medial VTA. *K–T*, TH immunoreactivity in the striatum. In *cNurr1*^{DATCre} mice, TH was lost in the CPu and diminished in the NAc. Scale bars, 250 μm.

modifications. Briefly, 25 μl of each sample were injected by a cooled autosampler (Midas) into an ESA Coulochem III coupled with an electrochemical detector. The mobile phase (5 g/L sodium acetate, 30 mg/L Na2-EDTA, 100 mg/L octane-sulfonic acid, and 10% methanol, pH 4.2) was delivered at a flow rate of 500 μl/min to a reverse-phase C18 column (4.6 mm diameter, 150 mm).

Fluorogold retrograde tracing. Animals received one unilateral stereotaxic injection in the right striatum using a 5 μl Hamilton microsyringe (22 gauge steel cannula) filled with the retrograde tracer Fluorogold (hydroxystilbamidine, 4%, Biotium). The animals were anesthetized with isoflurane, 0.5 μl was injected during 1 min, and the cannula was left in place for an additional 2 min before slowly being retracted. The anteroposterior and mediolateral coordinates from bregma were 0.27 and −2.10 mm, respectively, and the dorsoventral coordinates from the dura were −2.60 mm. Animals were killed 4 d after injection, and the brains were isolated. Fresh-frozen sections (14 μm) were cut with a cryostat and examined under a epifluorescence microscope (Eclipse E1000K; Nikon) coupled to an RTke spot camera.

Open-field test. This test was used to monitor overall activity and rearing behavior. The open field consisted of a white plastic box (55 × 35 × 30 cm) with lines (squares of 7 × 35 cm) painted on its floor. The animals were put in the center of the box, habituated for 10 min, and filmed 15 min thereafter while rearing was scored. The video recordings were used to measure the number of lines crossed during the monitoring period. A line crossing was counted when the mouse moved its whole body from one square to another.

Stepping test. Forelimb akinesia was monitored in a modified version of the stepping test, as described previously for rats (Schallert et al., 1992; Kirik et al., 1998). The test was performed three times daily over 3 consecutive days. In this test, the mouse was held firmly by the experimenter with both hindlimbs and one forelimb immobilized, and the mouse was passively moved with the free limb contacting a table surface. The number of adjusting steps, performed by the free forelimb when moved in the forehand and backhand directions, over a distance of 30 cm, was recorded. Results are presented as data collected on the third testing day.

Results

Selective *Nurr1* ablation in late developing mDA neurons

A mouse strain containing a *Nurr1* allele for conditional gene ablation was generated by insertion of two loxP sequences in the second and third introns so that the coding sequence, including the first coding exon 3, is excised by Cre-mediated recombination (supplemental Fig. 1, available at www.jneurosci.org as supplemental material). To analyze the consequences of *Nurr1* ablation at late stages of mDA neuron development, we crossed floxed *Nurr1* mice with mice carrying *Cre* inserted in the locus of the *DAT* gene (Ekstrand et al., 2007). Crosses generated *Nurr1* mice that were homozygous for the conditional targeted *Nurr1* allele and heterozygous for the *DAT–Cre* allele (*Nurr1*$^{L2/L2}$;*DAT*$^{Cre/wt}$; hereafter referred to as *cNurr1*^{DATCre} mice). Littermates of genotype *Nurr1*$^{L2/L2}$; *DAT*$^{wt/wt}$ or *Nurr1*$^{w/w}$;*DAT*$^{Cre/wt}$ were used as controls. Although we cannot exclude that a small number of cells escape Nurr1 gene deletion, immunohistochemistry using an antibody against Nurr1 showed that *DAT–Cre*-mediated *Nurr1* ablation resulted in the expected delayed loss of Nurr1 expression in mDA neurons beginning from approximately E13.5 and becomes essentially complete at E15.5 (supplemental Fig. 2, available at www.jneurosci.org as supplemental material). At this stage of normal development, cells express pan-neuronal properties as well as many mDA neuron markers, and axons are growing toward the developing striatum (Smidt and Burbach, 2007).

cNurr1^{DATCre} mice were born at the expected Mendelian frequency of ~25% (of a total $n = 159$); however, *cNurr1*^{DATCre} mice were less active than controls and did not survive beyond 3 weeks after birth. If litters were allowed to remain with their mothers after weaning, perinatal death was avoided in ~50% of *cNurr1*^{DATCre} pups. These surviving mice were, however, ~40% smaller than controls at the age of 2 months (supplemental Fig. 3, available at www.jneurosci.org as supplemental material). Although no significant change in spontaneous light-phase locomotor activity could be observed in adult *cNurr1*^{DATCre} mice, rearing was dramatically decreased (supplemental Fig. 3, available at www.jneurosci.org as supplemental material). L-DOPA treatment of mutant mice did not improve viability and did not induce any weight gain. Instead, *cNurr1*^{DATCre} mice display a pronounced and severe hypersensitivity to L-DOPA treatment characterized by an acute phase of hyperactivity and repetitive behaviors (including repetitive gnawing, excessive grooming, and self-injury) in all tested mutant ($n = 9$) but not in any wild-type controls ($n = 7$) (see Materials and Methods). These behaviors resemble those that have been observed in neonatal 6-hydoxydopadmine lesioned rats treated with L-DOPA (Breese et al., 2005). In conclusion, late embryonic mDA neuron-selective *Nurr1* ablation is associated with decreased weight, rearing, and viability, and mice show an altered response to L-DOPA.

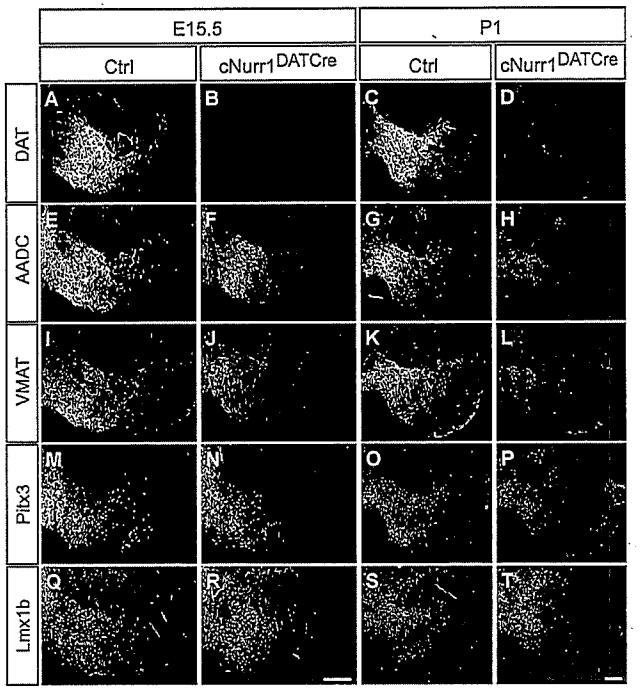

Figure 2. All analyzed mDA neuron markers are lost or diminished in *cNurr1*^{DATCre} mice. *A–T*, Confocal microscopy showing immunohistochemistry of several different mDA neuron markers in control (ctrl) and in *cNurr1*^{DATCre} mice at E15.5 or at P1, as indicated. The following markers were analyzed: DAT, AADC, VMAT, Pitx3, and Lmx1b. Results show a progressive loss of markers that is more substantial in the lateral SNc, whereas more medial VTA cells are lost more slowly. DAT is completely absent already at E15.5 in *cNurr1*^{DATCre} mice, whereas all other markers are decreased more slowly in this area (compare *A*, *B*). Scale bars, 200 μm.

Reduced levels of TH and DA in brains of *cNurr1*^{DATCre} mice

The observed abnormalities are consistent with a dopaminergic deficiency. To analyze the possible cellular basis for the phenotype, brain sections from controls and *cNurr1*^{DATCre} mice were analyzed by immunohistochemistry using an antibody against TH (Fig. 1). A progressive loss of TH immunostaining in SNc was observed in the *cNurr1*^{DATCre} mice (Fig. 1*A–J*). TH levels were significantly decreased already at E15.5, soon after Nurr1 is lost, and decreased further until adulthood when only scattered TH-positive neurons could be detected. TH was diminished also within the VTA at later stages, but a significant number of cells remained even in adult animals (Fig. 1*A–J*). These cells were counted in four nonconsecutive sections for each analyzed brain. In adult control VTA, a mean of 74.5 ± 7.1 cells per section were counted in *cNurr1*^{DATCre} mice ($n = 4$) and 499.3 ± 5.2 cells in controls ($n = 3$) (Student's t test, 4.4×10^{-7}). TH immunostaining within the caudatus putamen (CPu) was completely lost (Fig. 1*K–T*). However, weak immunoreactivity remained in nucleus accumbens (NAc) innervated preferentially by VTA neurons (Fig. 1*K–T*). We also noted the appearance of ectopic TH-positive cell bodies within the striatal parenchyma in *cNurr1*^{DATCre} mice (supplemental Fig. 4, available at www.jneurosci.org as supplemental material). These cells were more frequent in regions in which striatal TH had been most severely depleted as a consequence of Nurr1 ablation and resemble TH-positive neurons appearing in rodent and primate DA-depletion models (Huot and Parent, 2007). Decreased levels of TH immunostaining were paralleled by decreased DA levels, as measured by HPLC (supplemental Tables 1–3, available at www.jneurosci.org as supplemental material). Striatal DA was dramatically reduced to 14% of controls at P1 in *cNurr1*^{DATCre} mice and was almost completely lost by P60. An increased ratio of HVA to DA at P14 indicated increased turnover of DA in remaining cells at this stage (supplemental Table 2, available at www.jneurosci.org as supplemental material). DA was more severely decreased in CPu compared with NAc (supplemental Table 3, available at www.jneurosci.org as supplemental material). In contrast, 5-HT was significantly increased in both CPu and NAc, consistent with previous findings showing increased serotoniergic innervation after striatal DA depletion (Snyder et al., 1986). Thus, a severe neurotransmitter deficiency of the mesostriatal DA system is apparent in *cNurr1*^{DATCre} mice. Together, measurements of TH immunoreactivity and DA levels demonstrate that Nurr1 is critically required for maintaining TH expression and DA synthesis from late stages of mDA neuron differentiation.

Cellular deficiency within the ventral midbrain of *cNurr1*^{DATCre} mice

To investigate whether the phenotype is a consequence of a more limited disruption of DA synthesis or a more severe cellular deficiency, a number of additional mDA neuron markers were analyzed. All analyzed mDA neuron markers were diminished or absent within SNc in *cNurr1*^{DATCre} mice already at E15.5 (Fig. 2). DAT was completely lost at E15.5 and therefore, consistent with previous data (Sacchetti et al., 1999), stands out as being a likely direct target of Nurr1 (Fig. 2*A–D*). Additional control experiments showed that DAT and other markers, including TH and

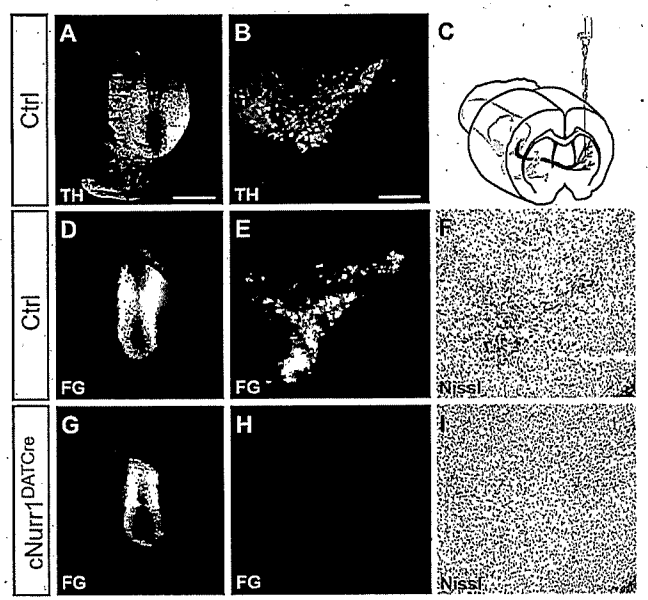

Figure 3. Cell bodies and striatal innervation are lost in $cNurr1^{DATCre}$ mice as determined by Fluorogold (FG) retrograde tracing of fibers extending from cell bodies in SNc to the striatum. *A–C*, After Fluorogold injection, injected into the left striatum in either adult (1.5 months old) control (Ctrl) or $cNurr1^{DATCre}$ mice as indicated in *C*, mice were killed after 4 d and analyzed for TH immunofluorescence in the striatum (*A*) or ventral midbrain (*B*). *D–I*, Analysis for Fluorogold (FG) or by Nissl staining. Strong Fluorogold staining in both striatum (*D*) and in the ventral midbrain (*E*) was consistently seen in all control (Ctrl) animals ($n = 7$). In contrast, Fluorogold fluorescence was only detected in the striatum (*G*) in $cNurr1^{DATCre}$ mice ($n = 5$), indicating that fibers from the SNc (*H*) had been lost in these animals. Moreover, large, densely packed cell bodies are only visualized by Nissl staining in the ventral midbrain of control animals (*F*) but are completely absent from $cNurr1^{DATCre}$ mice (*I*). Striatal site of Fluorogold injection is marked by asterisk in *A*, *D*, and *G*. Scale bars: *A*, *B*, *D*, *E*, *G*, *H*, 1 μm; *F*, *I*, 1200 μm.

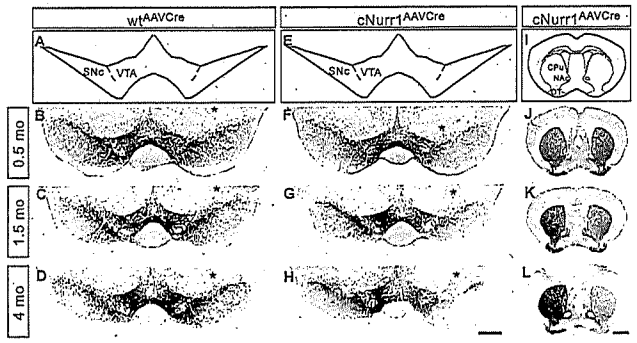

Figure 4. TH expression in both the ventral midbrain and striatum is progressively lost in the injected, but not non-injected, side of $cNurr1^{AAVCre}$ mice. *A–H*, Sections from 0.5, 1.5, and 4 month (mo; as indicated) old AAV–Cre-injected controls (wt^{AAVCre}) or $cNurr1^{AAVCre}$ mice were used for analyses by nonfluorescent DAB TH immunostaining in the ventral midbrain. The analyzed region within the ventral midbrain is schematically illustrated in *A* and *E*. The site of injection, marked by an asterisk in *B–D* and *F–H*, was verified in all animals by high-power magnification microscopy and was identified as a small area of injection-induced necrosis. Results show that TH immunostaining is not drastically altered at 0.5 months but is progressively decreased at 1.5 and 4 months in the injected SNc and VTA. *I–L*, DAB TH staining at the level of striatum. Analyzed regions are indicated in *I*. TH staining is progressively decreased at 1.5 and 4 months in the side that is ipsilateral to the side of AAV–Cre injection in $cNurr1^{AAVCre}$ mice (*J–L*). OT, Olfactory tubercle. Scale bars: *A–H*, 600 μm; *I–L*, 1 mm.

Nurr1, were not visibly decreased in mice heterozygous for the *DAT–Cre* allele (supplemental Fig. 5, available at www.jneurosci.org as supplemental material) (data not shown). In contrast to DAT, AADC, VMAT2, Pitx3, or Lmx1b were not reduced within the most medial ventral midbrain at this early stage and, with the exception of DAT, markers were not completely downregulated at P1 (Fig. 2*E–T*). The progressive loss of markers indicates a severe loss of phenotype within the SNc, whereas cells within the VTA appear more resilient. Importantly, most TH-positive cells within the VTA have lost any detectable expression of DAT, indicating that these cells have not escaped Nurr1 gene targeting (supplemental Fig. 6, available at www.jneurosci.org as supplemental material).

To further assess the extent of a cellular deficiency, striatal target innervation was analyzed by Fluorogold retrograde tracing after injection into the striatum of live 8- to 9-week-old controls and $cNurr1^{DATCre}$ mice. Fluorogold was transported into SNc cell bodies of control mice; however, fluorescence was entirely undetected within the SNc of Fluorogold-injected $cNurr1^{DATCre}$ mice (Fig. 3, compare *D*, *E* with *G*, *H*). In addition, characteristic large and densely packed TH-immunoreactive mDA neurons within the SNc were virtually absent in $cNurr1^{DATCre}$ mice (Fig. 3*I*). In conclusion, Nurr1 ablation in $cNurr1^{DATCre}$ mice results in rapid loss of SNc cell bodies; however, scattered VTA neurons remained even in adult $cNurr1^{DATCre}$ mice.

Adeno-associated virus–Cre-mediated *Nurr1* ablation in adult mice

In $cNurr1^{DATCre}$ mice, *Nurr1* is ablated well before full mDA neuron maturity and before targets in the striatum have become innervated; thus, it remained possible that the phenotype is a consequence of a developmental dysfunction. Therefore, we proceeded to inactivate *Nurr1* specifically in ventral midbrain of adult mice, using an adeno-associated virus (AAV)–Cre vector driven by the neuron-specific synapsin promoter. AAV–Cre was administered by unilateral stereotaxic microinjection above the right SNc. Cre immunohistochemistry and β-galactosidase expression was analyzed after intranigral AAV–Cre injection into reporter mice in which the ROSA26 locus is targeted with a LacZ reporter gene (Soriano, 1999). Results show widespread Cre expression around the site of injection, spreading into both SNc and VTA, and robust recombination of the LacZ reporter construct (supplemental Fig. 7, available at www.jneurosci.org as supplemental material). Moreover, except for a small necrotic area around the site of injection, virus administration did not affect tissue morphology, expression of mDA neuron markers, or microglia activation (data not shown).

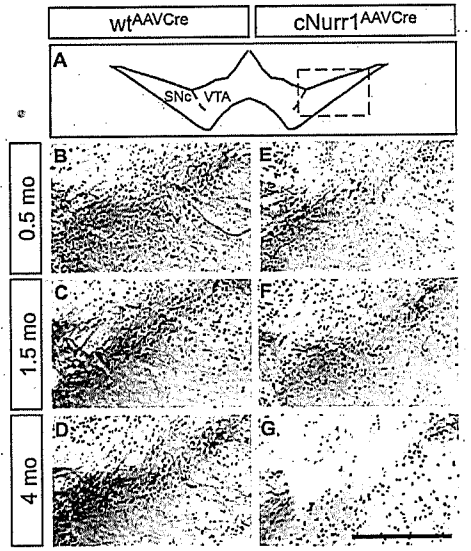

Figure 5. Cre-expressing cells are lost at 4 months within the SNc after Nurr1 ablation. *A*, Higher magnification showing TH by DAB staining (brown) at the level of the injected SNc in wt^{AAVCre} and $cNurr1^{AAVCre}$ mice. The region that has been magnified is boxed in *A*. *B–G*, Adjacent sections were Immunostained for Cre (black) and are superimposed on the DAB-stained TH sections in all micrographs. Cre staining is widespread in the area in which mDA neurons are normally localized at 0.5 and 1.5 months (*E*, *F*) but almost completely absent in this area at 4 months (*G*). Scale bar, 500 μm.

AAV–Cre was unilaterally injected above the SNc of adult mice homozygous for the floxed *Nurr1* allele to generate adult conditional gene-targeted mice ($cNurr1^{AAVCre}$) or into wild-type control mice (wt^{AAVCre}). In addition, a vector encoding the green fluorescent protein (GFP) driven by the synapsin promoter (AAV–GFP) was injected in mice homozygous for the floxed *Nurr1* allele ($cNurr1^{AAV-GFP}$ mice) to ensure that the floxed animals are not more sensitive to nonspecific toxicity induced by AAV transduction. Histological analyses were performed from animals killed at 0.5, 1.5, and 4 months after injection.

Reduction of TH and DA in adult *Nurr1*-ablated mice

TH immunohistochemistry at the level of the ventral midbrain was analyzed to assess the consequences of adult *Nurr1* ablation. Within SNc, TH immunoreactivity was unaffected at 0.5 months but was progressively reduced at 1.5 and 4 months in the injected SNc in $cNurr1^{AAVCre}$ mice (Fig. 4*E–H*). In contrast, TH immunoreactivity was unaffected in SNc of control wt^{AAVCre} and $cNurr1^{AAV-GFP}$ mice (Fig. 4*A–D*) (data not shown). TH was also reduced in the VTA at 1.5 and 4 months; however, at 4 months, the reduction in VTA was less dramatic compared with SNc (Fig. 4*E–H*).

Decreased striatal TH immunoreactivity paralleled the reduction in the ventral midbrain. Thus, although no signs of degenerating striatal TH-stained fibers (swollen axons or dystrophic neurites) were detected, striatal sections ipsilateral to the side of AAV–Cre injection showed clearly reduced TH in $cNurr1^{AAVCre}$ mice but not in controls (wt^{AAVCre} or $cNurr1^{AAV-GFP}$) (Fig. 4*I–L*) (supplemental Fig. 8, available at www.jneurosci.org as supplemental material). Diminished TH immunoreactivity was observed in regions innervated by both SNc and VTA (CPu and NAc, respectively), consistent with the reduced TH immunoreactivity in both SNc and VTA mDA neuron cell bodies. Measurement of DA and metabolites by HPLC from dissected tissue at 4 months confirmed this picture as a significant reduction in DA and DA metabolites noted both within the dorsolateral striatum and in areas mostly innervated by the VTA (cortex and ventromedial striatum) (supplemental Table 4, available at www.jneurosci.org as supplemental material). Thus, TH, DA, and DA metabolites are clearly reduced as a result of adult *Nurr1* ablation.

Loss of mDA neuron characteristics in adult *Nurr1*-ablated mice

To further analyze the fate of *Nurr1*-ablated neurons, cells were counted within the SNc and VTA in $cNurr1^{AAVCre}$ and wt^{AAVCre} mice. Within SNc, the number of TH-positive cells was significantly decreased at 4 months (58.1 ± 8.3 and 95.4 ± 6.3% in the injected vs non-injected sides of $cNurr1^{AAVCre}$ and wt^{AAVCre} mice, respectively; $p = 0.0053$). In contrast, the numbers of TH-positive cells was not significantly reduced within the VTA (104.1 ± 4.7 and 101.6 ± 10.5% in the injected versus non-injected sides of $cNurr1^{AAVCre}$ and wt^{AAVCre} mice, respectively). Also, the numbers of TH-positive cells were not significantly changed in $cNurr1^{AAVCre}$ mice at 1.5 months (data not shown).

To assess the integrity of neurons, cellular analysis was extended by analyzing Cre-immunolabeled sections that were superimposed on adjacent TH-labeled sections (Fig. 5). Notably, in $cNurr1^{AAVCre}$ mice, Cre expression was clearly detected within the area of SNc at both 0.5 and 1.5 months but was lost at 4 months in the region in which mDA neurons should normally be localized (Fig. 5, compare *E–G* with *B–D*). Cre expression is driven by a general neuronal promoter (synapsin), suggesting that loss of Nurr1 may eventually affect some pan-neuronal properties at 4 months after ablation.

Confocal microscopy confirmed the loss of TH at 1.5 and 4 months after Nurr1 ablation and the loss of Cre at 4 months (Fig. 6*A–D*). At 1.5 months, DAT expression was weak but cell bodies were readily identified (Fig. 6*E*,*F* and inset in *F*). DAT staining remained also at 4 months, but, at this stage, high-power magnification indicated that some of the staining appeared confined to fibers and/or dystrophic cells (Fig. 6*G*,*H* and inset in *H*). Nonetheless, at 4 months, most cells with decreased TH stained positive for AADC, showing that not all mDA neuron characteristics were affected (Fig. 7*A–F*). Moreover, VMAT2 is yet another marker that was severely decreased in $cNurr1^{AAVCre}$ mice, but remaining weakly stained cells were positive for the general neuronal marker Hu (Fig. 7*G–L*). The observed changes were not correlated to increased number of apoptotic cells because increased activated Caspase 3 could not be detected (data not shown). Also, we found no evidence for nigral inflammation or α-synucleinopathy because activated microglia and α-synuclein-rich inclusions were not detected at any stage after Nurr1 ablation in $cNurr1^{DATCre}$ mice (data not shown). Finally, TH and DAT expression in VTA was also affected, without any apparent loss of the neuronal marker Hu or any signs of dystrophic cells (supplemental Fig. 9, available at www.jneurosci.org as supplemental material) (data not shown). Thus, Nurr1 ablation results in a

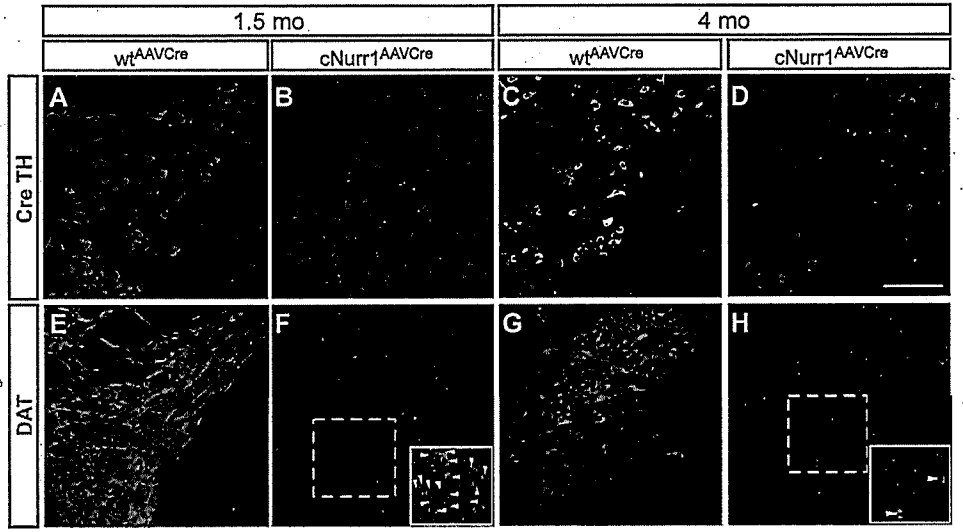

Figure 6. Decreased expression of DAT and signs of dystrophic cells in $cNurr1^{AAVCre}$ mice. *A–H*, Confocal analysis of SNc in wt^{AAVCre} and $cNurr1^{AAVCre}$ mice at 1.5 and 4 months, as indicated. Confocal images show double staining of Cre (red) and TH (green; *A–D*) and staining for DAT (green; *E–H*). Micrographs show that there is a loss of TH and DAT and a progressive loss of synapsin-driven Cre at 4 months. At 4 months, DAT staining appears fragmented and stains scattered fibers, whereas very few intact cell profiles (marked with arrowheads in *F* and *H*) can be identified in $cNurr1^{AAVCre}$ mice (compare insets in *F*, *H*). Scale bar, 200 μm.

progressive dysfunction characterized by a partial loss of the mDA neuron phenotype. Although we see few signs of neuronal degeneration, we cannot exclude a limited cell loss.

To assess whether the observed dysfunction was paralleled by an altered motor behavior, $cNurr1^{AAVCre}$ mice were subjected to a stepping test at 3 and 4 months (Schallert et al., 1992; Kirik et al., 1998). Performance of the left forelimb (i.e., the limb contralateral to the vector injection) was impaired at both time points (Fig. 8). Additional behavioral testing, including amphetamine-induced rotations and a corridor test, indicated that individual mutant animals appeared affected; however, the *Nurr1*-ablated group did not show alterations that were statistically significant (supplemental Fig. 10, available at www.jneurosci.org as supplemental material). Our results demonstrate progressive mDA neuron dysfunction, leading to a more severe deficiency at 3–4 months after *Nurr1* ablation.

Discussion

This study provides definitive evidence that Nurr1 is not only critical for early differentiation but also for the maintenance of functional mDA neurons. Conditional gene targeting at late embryogenesis, when characteristic features of mDA neurons are already apparent, results in a rapid and close to complete mDA neuron loss. Only few TH-positive cells remain within the VTA also in the absence of Nurr1. Removal of Nurr1 leads to a severe dysfunction also in adult mDA neurons. It should be noted that reduction of striatal DA and the behavioral effects after adult ablation most likely underestimate the importance of Nurr1 in the adult brain because AAV injection only transduced a proportion of all mDA neurons in the injected side of treated animals. Thus, these data emphasize the importance of studying developmental mechanisms for elucidating neuron maintenance mechanisms. An analogous example is provided by the glial cell line-derived neurotrophic factor (GDNF). GDNF is known to promote neuronal survival under development, but only recently has conditional gene targeting enabled studies that interrogate the role of GDNF and other factors signaling via Ret for maintenance of midbrain dopamine neurons in the adult brain (Oo et al., 2003; Jain et al., 2006; Kramer et al., 2007; Pascual et al., 2008).

Data presented here have implications for our understanding of how mature differentiated cell types are maintained. Previous studies have indicated that the differentiated state is not irreversible because even mature specialized cells, including for example, olfactory neurons and mature T- and B-cells, can be reprogrammed into undifferentiated pluripotent cells by either somatic cell nuclear transfer or using the recently developed methodology for the generation of induced pluripotent stem cells (Takahashi and Yamanaka, 2006; Gurdon and Melton, 2008). Nevertheless, under normal nonmanipulated conditions *in vivo*, differentiated cells are remarkably stable, indicating the importance of mechanisms that maintain cells in their appropriate differentiated state. Gene targeting in non-neural cell types has revealed how transcription factors functioning in development can be important for the maintenance of terminally differentiated cell types, e.g., Pax5 in B-lymphocytes and Prox1 in lymphatic endothelial cells (Cobaleda et al., 2007; Johnson et al., 2008). In CNS, transcription factors identified for their key roles in early neuron development often continue to be expressed in the adult brain and may therefore guard against loss of phenotype or drift into alternative states (Smidt et al., 1997, 2000; Zetterström et al., 1997; Hendricks et al., 1999; Vult von Steyern et al., 1999; Albéri et al., 2004; Simon et al., 2004; Kang et al., 2007; Kittappa et al., 2007; Smidt and Burbach, 2007; Alavian et al., 2008). However, remarkably little is known of how these factors function at late stages of development or in the adult. Although examples of adult mDA neuron loss has been reported in mice haploinsufficient for transcription factor genes such as *Engrailed* and *FoxA2*, it remains possible that defects originate during embryonic development (Albéri et al., 2004; Zhao et al., 2006; Kittappa et al., 2007; Sonnier et al., 2007). Importantly, FoxA2 and Engrailed are critical for the establishment of the floor plate and for early midbrain/hindbrain development, respectively, and they are directly and indirectly affecting many cell fates along the entire neuraxis. Thus, haploinsufficiency may cause embryonal deficiencies that do not become manifest until adult stages, a possibility that emphasizes the importance of temporally controlled conditional gene targeting to rigorously test how transcription factors function in terminally differentiated neurons.

We do not yet understand why Nurr1 is required in already differentiated mDA neurons. However, data presented here provide compelling evidence for the existence of "terminal selector genes" in mammalian CNS development. Such genes, defined from studies of *Caenorhabditis elegans* neuronal development, are continuously expressed throughout the life of neurons and are essential for both the establishment and maintenance of distinct neuronal phenotypes (Hobert, 2008). Thus, Nurr1, which probably regulates typical mDA neuron markers such as *TH*, *DAT*, *AADC*, and *VMAT2* (Sakurada et al., 1999; Sacchetti et al., 2001; Hermanson et al., 2003; Kim et al., 2003), is likely required for both early differentiation and maintenance by regulating genes that distinguish mDA neurons from other neuron types. Presumably, such regulation is critical throughout the life of mDA neurons and would depend on additional components, such as Pitx3, in a core transcription factor network (Jacobs et al., 2009).

How may dysregulated Nurr1 activity contribute to PD? Studies in PD patients have shown that, in early stages of the disease, SNc cell bodies are relatively spared compared with the loss of DA in the putamen (Fearnley and Lees, 1991) and that a significant fraction of the surviving, pigmented, DA somata in the SNc have much reduced expression of the TH enzyme (Hirsch et al., 1988; Chu et al., 2006). This suggests that, during early stages of disease, nigral DA neurons may survive in a dysfunctional state characterized by a downregulated neurotransmitter machinery. An interesting possibility supported by our data is that reduced expression of Nurr1 contributes to such symptoms. Indeed, Nurr1 is severely reduced in neurons with signs of pathology in PD brain tissue, and reduced Nurr1 expression in patients' peripheral blood lymphocytes indicates that diminished Nurr1 activity may be a systemic feature of disease (Chu et al., 2006; Le et al., 2008). Although such correlations do not determine whether reduced Nurr1 expression is a cause or a consequence of disease, progressive cell dysfunction in *Nurr1*-ablated mice provides a clear indication that diminished Nurr1 expression in PD should have deleterious consequences for patients. This view is supported by the identification of *Nurr1* gene variants that have been associated with rare cases of familial and sporadic PD (Xu et al., 2002; Le et al., 2003; Zheng et al., 2003; Jankovic et al., 2005; Grimes et al., 2006; Jacobsen et al., 2008). Although other studies have failed to identify such mutations and indicated that Nurr1

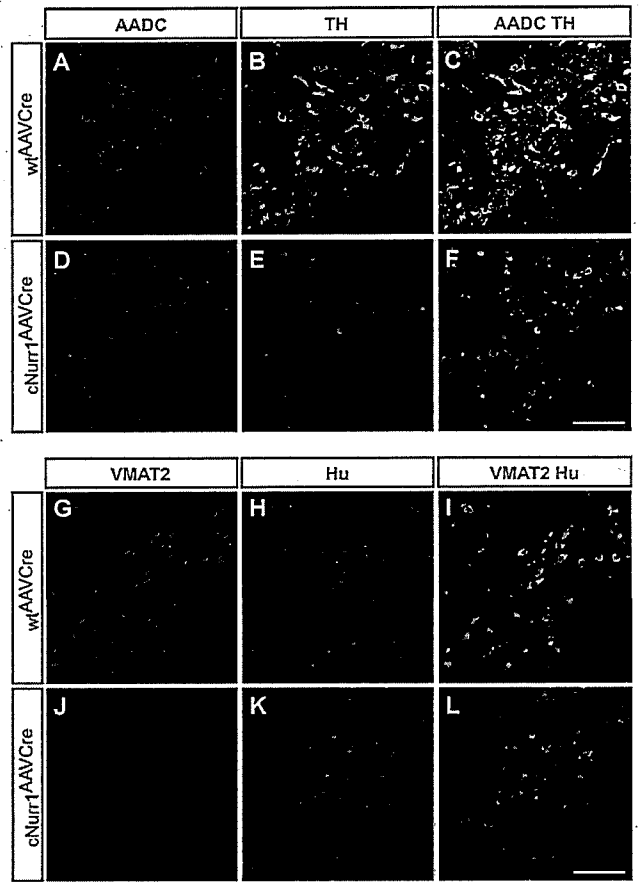

Figure 7. Decreased levels of VMAT2 but not AADC in $cNurr1^{AAVCre}$ mice. Confocal analysis of SNc in wt^{AAVCre} and $cNurr1^{AAVCre}$ mice at 4 months, as indicated. *A–F*, Confocal images show staining of AADC (red; *A*, *D*), TH (green; *B*, *E*), and double staining of both markers (*C*, *F*). Micrographs show that AADC expression appears expressed at normal levels in most cells with decreased levels of TH. *G–L*, Confocal images show staining for VMAT2 (red; *G*, *J*), Hu (*H*, *K*), and double staining of both markers (*I*, *L*). Micrographs show that VMAT2 is severely decreased in $cNurr1^{AAVCre}$ mice, whereas Hu is maintained at normal levels in essentially all cells with decreased VMAT2. Scale bar, 200 μm.

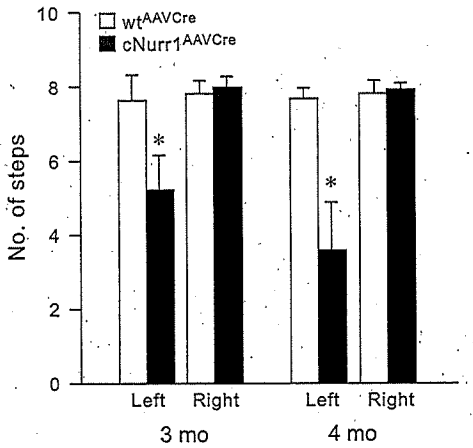

Figure 8. Forelimb akinesia in the stepping test. The performance of the left paw (contralateral to the vector injection) was significantly impaired in the fl/fl mice ($n = 16$) but not the wild-type mice ($n = 13$). Although the impairment was significant at both time points, 3 and 4 months after vector injection, their performance got significantly worse over time ($p < 0.01$, Student's paired t test): 15 of the 16 mice in the fl/fl group showed a decline in their stepping scores between the two tests, and at 4 months, 14 of the fl/fl mice had scores below 5 compared with 6 in the 3 month test. Scores give the means of steps recorded in the forehand and backhand direction for each paw (see Materials and Methods). *$p < 0.001$, Student's paired t test.

gene variants as a cause of PD must be very rare, the combined data from genetics, postmortem PD brain tissue analyses, and the ablation experiments reported here strongly imply that, if and when Nurr1 function is reduced, it will exaggerate PD progression and severity (Wellenbrock et al., 2003; Hering et al., 2004; Tan et al., 2004).

The results indicate that therapies that can restore Nurr1 activity in diseased but not yet degenerated mDA neurons could be of clinical relevance. We envision several strategies whereby Nurr1 activity could be increased. (1) Nurr1 belongs to the nuclear receptor family whose members are commonly regulated by small lipophilic ligands. The putative ligand binding domain of Nurr1 is unconventional and lacks a ligand-binding pocket, but Nurr1 forms heterodimers with retinoid X receptors (RXRs), and ligands activating these receptors can protect mDA neurons in culture (Wallen-Mackenzie et al., 2003; Wang et al., 2003). Thus, RXR may be a relevant target for ligand modulation of Nurr1-regulated processes. It will be important to investigate to what extent Nurr1–RXR heterodimers versus Nurr1 alone are important in pathways associated with the phenotype described in this paper. (2) Nurr1 activity is possible to modulate, for example, by the leukemia drug 6-mercaptopurine (Ordentlich et al., 2003). Although such drugs are pleiotropic and serious side effects are likely, other compounds with higher specificity may be possible to identify. (3) Therapies directed at increasing Nurr1 activity would be effective only as long as sufficient levels of Nurr1 are expressed in diseased neurons. Thus, treatments aimed at restoration of Nurr1 expression by gene delivery may prove advantageous. Using similar AAV vectors as administered in this study may be of particular interest because they have properties that are clinically favorable and are already used in clinical trials in PD patients (Check, 2007).

In conclusion, loss of Nurr1 at stages when characteristic features of mDA neurons are already apparent in the developing embryo or in fully differentiated adult neurons results in loss of mDA neuron-specific gene expression and neuron degeneration. These findings highlight the importance of developmental mechanisms also in the adult brain and clearly indicate that they may be critical for the understanding of cell maintenance and neurodegeneration. How Nurr1 and other transcription factors operate in adult neurons to control and prevent loss or drift in phenotype remains a challenge for future studies.

References

Alavian KN, Scholz C, Simon HH (2008) Transcriptional regulation of mesencephalic dopaminergic neurons: the full circle of life and death. Mov Disord 23:319–328.

Albéri L, Sgadò P, Simon HH (2004) Engrailed genes are cell-autonomously required to prevent apoptosis in mesencephalic dopaminergic neurons. Development 131:3229–3236.

Andersson E, Tryggvason U, Deng Q, Friling S, Alekseenko Z, Robert B, Perlmann T, Ericson J (2006) Identification of intrinsic determinants of midbrain dopamine neurons. Cell 124:393–405.

Breese GR, Knapp DJ, Criswell HE, Moy SS, Papadeas ST, Blake BL (2005) The neonate-6-hydroxydopamine-lesioned rat: a model for clinical neuroscience and neurobiological principles. Brain Res Brain Res Rev 48:57–73.

Castillo SO, Baffi JS, Palkovits M, Goldstein DS, Kopin IJ, Witta J, Magnuson MA, Nikodem VM (1998) Dopamine biosynthesis is selectively abolished in substantia nigra ventral tegmental area but not in hypothalamic neurons in mice with targeted disruption of the Nurr1 gene. Mol Cell Neurosci 11:36–46.

Check E (2007) Second chance. Nat Med 13:770–771.

Chu Y, Le W, Kompoliti K, Jankovic J, Mufson EJ, Kordower JH (2006) Nurr1 in Parkinson's disease and related disorders. J Comp Neurol 494:495–514.

Cobaleda C, Jochum W, Busslinger M (2007) Conversion of mature B cells into T cells by dedifferentiation to uncommitted progenitors. Nature 449:473–477.

Ekstrand MI, Terzioglu M, Galter D, Zhu S, Hofstetter C, Lindqvist E, Thams S, Bergstrand A, Hansson FS, Trifunovic A, Hoffer B, Cullheim S, Mohammed AH, Olson L, Larsson NG (2007) Progressive parkinsonism in mice with respiratory-chain-deficient dopamine neurons. Proc Natl Acad Sci U S A 104:1325–1330.

Fearnley JM, Lees AJ (1991) Ageing and Parkinson's disease: substantia nigra regional selectivity. Brain 114:2283–2301.

Grimes DA, Han F, Panisset M, Racacho L, Xiao F, Zou R, Westaff K, Bulman DE (2006) Translated mutation in the Nurr1 gene as a cause for Parkinson's disease. Mov Disord 21:906–909.

Gurdon JB, Melton DA (2008) Nuclear reprogramming in cells. Science 322:1811–1815.

Hendricks T, Francis N, Fyodorov D, Deneris ES (1999) The ETS domain factor Pet-1 is an early and precise marker of central serotonin neurons and interacts with a conserved element in serotonergic genes. J Neurosci 19:10348–10356.

Hering R, Petrovic S, Mietz EM, Holzmann C, Berg D, Bauer P, Woitalla D, Müller T, Berger K, Krüger R, Riess O (2004) Extended mutation analysis and association studies of Nurr1 (NR4A2) in Parkinson disease. Neurology 62:1231–1232.

Hermanson E, Joseph B, Castro D, Lindqvist E, Aarnisalo P, Wallén A, Benoit G, Hengerer B, Olson L, Perlmann T (2003) Nurr1 regulates dopamine synthesis and storage in MN9D dopamine cells. Exp Cell Res 288:324–334.

Hirsch E, Graybiel AM, Agid YA (1988) Melanized dopaminergic neurons are differentially susceptible to degeneration in Parkinson's disease. Nature 334:345–348.

Hobert O (2008) Regulatory logic of neuronal diversity: terminal selector genes and selector motifs. Proc Natl Acad Sci U S A 105:20067–20071.

Huot P, Parent A (2007) Dopaminergic neurons intrinsic to the striatum. J Neurochem 101:1441–1447.

Jacobs FM, van Erp S, van der Linden AJ, von Oerthel L, Burbach JP, Smidt MP (2009) Pitx3 potentiates Nurr1 in dopamine neuron terminal differentiation through release of SMRT-mediated repression. Development 136:531–540.

Jacobsen KX, MacDonald H, Lemonde S, Daigle M, Grimes DA, Bulman DE, Albert PR (2008) A Nurr1 point mutant, implicated in Parkinson's disease, uncouples ERK1/2-dependent regulation of tyrosine hydroxylase transcription. Neurobiol Dis 29:117–122.

Jain S, Golden JP, Wozniak D, Pehek E, Johnson EM Jr, Milbrandt J (2006) RET is dispensable for maintenance of midbrain dopaminergic neurons in adult mice. J Neurosci 26:11230–11238.

Jankovic J, Chen S, Le WD (2005) The role of Nurr1 in the development of dopaminergic neurons and Parkinson's disease. Prog Neurobiol 77:128–138.

Johnson NC, Dillard ME, Baluk P, McDonald DM, Harvey NL, Frase SL, Oliver G (2008) Lymphatic endothelial cell identity is reversible and its maintenance requires Prox1 activity. Genes Dev 22:3282–3291.

Kang BJ, Chang DA, Mackay DD, West GH, Moreira TS, Takakura AC, Gwilt JM, Guyenet PG, Stornetta RL (2007) Central nervous system distribution of the transcription factor Phox2b in the adult rat. J Comp Neurol 503:627–641.

Kim KS, Kim CH, Hwang DY, Seo H, Chung S, Hong SJ, Lim JK, Anderson T, Isacson O (2003) Orphan nuclear receptor Nurr1 directly transactivates the promoter activity of the tyrosine hydroxylase gene in a cell-specific manner. J Neurochem 85:622–634.

Kirik D, Rosenblad C, Björklund A (1998) Characterization of behavioral and neurodegenerative changes following partial lesions of the nigrostriatal dopamine system induced by intrastriatal 6-hydroxydopamine in the rat. Exp Neurol 152:259–277.

Kittappa R, Chang WW, Awatramani RB, McKay RD (2007) The foxa2 gene controls the birth and spontaneous degeneration of dopamine neurons in old age. PLoS Biol 5:e325.

Kramer ER, Aron L, Ramakers GM, Seitz S, Zhuang X, Beyer K, Smidt MP, Klein R (2007) Absence of Ret signaling in mice causes progressive and late degeneration of the nigrostriatal system. PLoS Biol 5:e39.

Le W, Pan T, Huang M, Xu P, Xie W, Zhu W, Zhang X, Deng H, Jankovic J (2008) Decreased NURR1 gene expression in patients with Parkinson's disease. J Neurol Sci 273:29–33.

Le WD, Xu P, Jankovic J, Jiang H, Appel SH, Smith RG, Vassilatis DK (2003) Mutations in NR4A2 associated with familial Parkinson disease. Nat Genet 33:85–89.

Oo TF, Kholodilov N, Burke RE (2003) Regulation of natural cell death in dopaminergic neurons of the substantia nigra by striatal glial cell line-derived neurotrophic factor *in vivo*. J Neurosci 23:5141–5148.

Ordentlich P, Yan Y, Zhou S, Heyman RA (2003) Identification of the antineoplastic agent 6-mercaptopurine as an activator of the orphan nuclear hormone receptor Nurr1. J Biol Chem 278:24791–24799.

Pascual A, Hidalgo-Figueroa M, Piruat JI, Pintado CO, Gómez-Díaz R, López-Barneo J (2008) Absolute requirement of GDNF for adult catecholaminergic neuron survival. Nat Neurosci 11:755–761.

Perlmann T, Wallén-Mackenzie A (2004) Nurr1, an orphan nuclear receptor with essential functions in developing dopamine cells. Cell Tissue Res 318:45–52.

Sacchetti P, Brownschidle LA, Granneman JG, Bannon MJ (1999) Characterization of the 5′-flanking region of the human dopamine transporter gene. Brain Res Mol Brain Res 74:167–174.

Sacchetti P, Mitchell TR, Granneman JG, Bannon MJ (2001) Nurr1 enhances transcription of the human dopamine transporter gene through a novel mechanism. J Neurochem 76:1565–1572.

Sakurada K, Ohshima-Sakurada M, Palmer TD, Gage FH (1999) Nurr1, an orphan nuclear receptor, is a transcriptional activator of endogenous tyrosine hydroxylase in neural progenitor cells derived from the adult brain. Development 126:4017–4026.

Saucedo-Cardenas O, Quintana-Hau JD, Le WD, Smidt MP, Cox JJ, De Mayo F, Burbach JP, Conneely OM (1998) Nurr1 is essential for the induction of the dopaminergic phenotype and the survival of ventral mesencephalic late dopaminergic precursor neurons. Proc Natl Acad Sci U S A 95:4013–4018.

Schallert T, Norton D, Jones TA (1992) A clinically relevant unilateral rat model of Parkinsonian akinesia. J Neural Transpl Plast 3:332–333.

Simon HH, Thuret S, Alberi L (2004) Midbrain dopaminergic neurons: control of their cell fate by the engrailed transcription factors. Cell Tissue Res 318:53–61.

Smidt MP, Burbach JP (2007) How to make a mesodiencephalic dopaminergic neuron. Nat Rev Neurosci 8:21–32.

Smidt MP, van Schaick HS, Lanctôt C, Tremblay JJ, Cox JJ, van der Kleij AA, Wolterink G, Drouin J, Burbach JP (1997) A homeodomain gene Ptx3 has highly restricted brain expression in mesencephalic dopaminergic neurons. Proc Natl Acad Sci U S A 94:13305–13310.

Smidt MP, Asbreuk CH, Cox JJ, Chen H, Johnson RL, Burbach JP (2000) A second independent pathway for development of mesencephalic dopaminergic neurons requires Lmx1b. Nat Neurosci 3:337–341.

Smidt MP, Smits SM, Burbach JP (2004) Homeobox gene Pitx3 and its role in the development of dopamine neurons of the substantia nigra. Cell Tissue Res 318:35–43.

Snyder AM, Zigmond MJ, Lund RD (1986) Sprouting of serotoninergic afferents into striatum after dopamine-depleting lesions in infant rats: a retrograde transport and immunocytochemical study. J Comp Neurol 245:274–281.

Sonnier L, Le Pen G, Hartmann A, Bizot JC, Trovero F, Krebs MO, Prochiantz A (2007) Progressive loss of dopaminergic neurons in the ventral midbrain of adult mice heterozygote for Engrailed 1. J Neurosci 27:1063–1071.

Soriano P (1999) Generalized lacZ expression with the ROSA26 Cre reporter strain. Nat Genet 21:70–71.

Takahashi K, Yamanaka S (2006) Induction of pluripotent stem cells from mouse embryonic and adult fibroblast cultures by defined factors. Cell 126:663–676.

Tan EK, Chung H, Chandran VR, Tan C, Shen H, Yew K, Pavanni R, Puvan KA, Wong MC, Teoh ML, Yih Y, Zhao Y (2004) Nurr1 mutational screen in Parkinson's disease. Mov Disord 19:1503–1505.

Vult von Steyern F, Martinov V, Rabben I, Njå A, de Lapeyrière O, Lømo T (1999) The homeodomain transcription factors Islet 1 and HB9 are expressed in adult alpha and gamma motoneurons identified by selective retrograde tracing. Eur J Neurosci 11:2093–2102.

Wallen-Mackenzie A, Mata de Urquiza A, Petersson S, Rodriguez FJ, Friling S, Wagner J, Ordentlich P, Lengqvist J, Heyman RA, Arenas E, Perlmann T (2003) Nurr1-RXR heterodimers mediate RXR ligand-induced signaling in neuronal cells. Genes Dev 17:3036–3047.

Wang Z, Benoit G, Liu J, Prasad S, Aarnisalo P, Liu X, Xu H, Walker NP, Perlmann T (2003) Structure and function of Nurr1 identifies a class of ligand-independent nuclear receptors. Nature 423:555–560.

Wellenbrock C, Hedrich K, Schafer N, Kasten M, Jacobs H, Schwinger E, Hagenah J, Pramstaller PP, Vieregge P, Klein C (2003) NR4A2 mutations are rare among European patients with familial Parkinson's disease. Ann Neurol 54:415.

Xu PY, Liang R, Jankovic J, Hunter C, Zeng YX, Ashizawa T, Lai D, Le WD (2002) Association of homozygous 7048G7049 variant in the intron six of Nurr1 gene with Parkinson's disease. Neurology 58:881–884.

Zetterström RH, Williams R, Perlmann T, Olson L (1996) Cellular expression of the immediate early transcription factors Nurr1 and NGFI-B suggests a gene regulatory role in several brain regions including the nigrostriatal dopamine system. Brain Res Mol Brain Res 41:111–120.

Zetterström RH, Solomin L, Jansson L, Hoffer BJ, Olson L, Perlmann T (1997) Dopamine neuron agenesis in Nurr1-deficient mice. Science 276:248–250.

Zhao ZQ, Scott M, Chiechio S, Wang JS, Renner KJ, Gereau RW 4th, Johnson RL, Deneris ES, Chen ZF (2006) Lmx1b is required for maintenance of central serotonergic neurons and mice lacking central serotonergic system exhibit normal locomotor activity. J Neurosci 26:12781–12788.

Zheng K, Heydari B, Simon DK (2003) A common NURR1 polymorphism associated with Parkinson disease and diffuse Lewy body disease. Arch Neurol 60:722–725.

J Physiol 587.20 (2009) pp 4845–4862

Primary motor cortical metaplasticity induced by priming over the supplementary motor area

Masashi Hamada[1], Ritsuko Hanajima[1], Yasuo Terao[1], Shingo Okabe[1], Setsu Nakatani-Enomoto[2], Toshiaki Furubayashi[2], Hideyuki Matsumoto[1], Yuichiro Shirota[1], Shinya Ohminami[1] and Yoshikazu Ugawa[2]

[1]*Department of Neurology, Division of Neuroscience, Graduate School of Medicine, The University of Tokyo, Tokyo, Japan*
[2]*Department of Neurology, School of Medicine, Fukushima Medical University, Fukushima, Japan*

Motor cortical plasticity induced by repetitive transcranial magnetic stimulation (rTMS) sometimes depends on the prior history of neuronal activity. These effects of preceding stimulation on subsequent rTMS-induced plasticity have been suggested to share a similar mechanism to that of metaplasticity, a homeostatic regulation of synaptic plasticity. To explore metaplasticity in humans, many investigations have used designs in which both priming and conditioning are applied over the primary motor cortex (M1), but the effects of priming stimulation over other motor-related cortical areas have not been well documented. Since the supplementary motor area (SMA) has anatomical and functional cortico-cortical connections with M1, here we studied the homeostatic effects of priming stimulation over the SMA on subsequent rTMS-induced plasticity of M1. For priming and subsequent conditioning, we employed a new rTMS protocol, quadripulse stimulation (QPS), which produces a broad range of motor cortical plasticity depending on the interval of the pulses within a burst. The plastic changes induced by QPS at various intervals were altered by priming stimulation over the SMA, which did not change motor-evoked potential sizes on its own but specifically modulated the excitatory I-wave circuits. The data support the view that the homeostatic changes are mediated via mechanisms of metaplasticity and highlight an important interplay between M1 and SMA regarding homeostatic plasticity in humans.

(Received 21 July 2009; accepted after revision 31 August 2009; first published online 1 September 2009)
Corresponding author M. Hamada: Department of Neurology, Division of Neuroscience, Graduate School of Medicine, The University of Tokyo, 7-3-1, Hongo, Bunkyo-ku, Tokyo 113-8655, Japan. Email: mhamada-tky@umin.net

Abbreviations CS, conditioning stimulus; FDI, first dorsal interosseous muscle; ICF, intracortical facilitation; ISI, inter-stimulus intervals; ITT, inter-train interval; LICI, long-interval intracortical inhibition; LTD, long-term depression; LTP, long-term potentiation; M1, primary motor cortex; MEP, motor-evoked potential; PMd and PMv, dorsal and ventral premotor cortex; QPS, quadripulse stimulation; rTMS, repetitive transcranial magnetic stimulation; SICF, short-interval intracortical facilitation; SICI, short-interval intracortical inhibition; SMA, supplementary motor area; TA, right tibialis anterior muscle; TS, test stimulus.

Introduction

Repetitive transcranial magnetic stimulation (rTMS) is a promising method to induce plastic changes in humans (Hallett, 2007). In some cases, the rTMS-induced plasticity is *N*-methyl-D-aspartate (NMDA) dependent, supporting the idea that changes in synaptic efficacy, such as long-term potentiation (LTP) and long-term depression (LTD), are implicated in rTMS-induced plasticity (Stefan *et al.* 2002; Huang *et al.* 2007). Several human studies have also shown effects of a prior history of neuronal activity on subsequent rTMS-induced plasticity (e.g. Siebner *et al.* 2004; Hamada *et al.* 2008*a*). These findings have been compared with metaplasticity, homeostatic regulation of synaptic plasticity in which the capacity of synapses to exhibit plasticity depends on prior levels of neuronal activity (Abraham & Bear, 1996; Ziemann & Siebner, 2008). This form of plasticity regulation might relate directly to the Bienenstock–Cooper–Munro (BCM) theory, a prevailing model for homeostatic mechanisms of synaptic plasticity (Bienenstock *et al.* 1982; Abraham, 2008).

The protocol for studying metaplasticity in an experimental context is to apply a period of priming stimulation (which on its own has little or no effect on synaptic plasticity) and then to test whether this changes the response to a second period of conditioning stimulation which produces LTP or LTD when given alone (Abraham, 2008). Many human studies have used designs in which both priming and conditioning are applied over the primary motor cortex (M1) (Iyer *et al.* 2003; Siebner *et al.* 2004; Lang *et al.* 2004; Müller *et al.* 2007; Hamada *et al.* 2008*a*). Others showed that metaplastic effects can be elicited by finger movements or voluntary muscle contraction, in place of priming stimulation, which might be associated with activity changes in cortical circuits within various motor-related areas (Ziemann *et al.* 2004; Gentner *et al.* 2008; Huang *et al.* 2008). More recently, Ragert *et al.* (2009) demonstrated the effects of priming stimulation over the right M1 on subsequent rTMS-induced plasticity of left M1 (Ragert *et al.* 2009). Of note is the fact that the effects of priming stimulation over motor-related areas other than ipsilateral or contralateral M1 have not been well documented, despite important anatomical and functional interplay between those areas and M1.

Among the motor-related areas, the lateral premotor cortex (PM) such as dorsal and ventral PM (PMd and PMv) has been extensively studied by means of TMS in humans to shed light on the interaction between M1 (see review by Reis *et al.* 2008). The supplementary motor area (SMA) also has dense cortico-cortical connections with M1 in animals (Dum & Strick, 1991; Luppino *et al.* 1993; Tokuno & Nambu, 2000) and plays a substantial role in higher motor control and learning (Tanji & Shima, 1994; Hikosaka *et al.* 1999; Nachev *et al.* 2008). However, as SMA is located in the interhemispheric fissure, it is a more difficult site to stimulate than the lateral PM (Reis *et al.* 2008). Thus, not much has been done in SMA as compared to PMd; two studies revealed that TMS over SMA can modulate the cortical excitability of M1 via cortico-cortical synaptic connections (Civardi *et al.* 2001; Matsunaga *et al.* 2005). In light of this accruing evidence, we aimed to explore the effects of preceding stimulation over SMA on subsequent rTMS-induced plasticity of the M1 in order to test the hypothesis that priming over the SMA modulates some cortical neurons within M1 via cortico-cortical connections, and that such prior history of neuronal activity alters subsequent rTMS-induced plasticity.

For priming and subsequent conditioning, we employed a new rTMS protocol, quadripulse stimulation (QPS) (Hamada *et al.* 2007, 2008*a*). QPS consists of repeated trains of four monophasic TMS pulses separated by inter-stimulus intervals (ISI) of 1.5–1250 ms, inducing bidirectional motor cortical plasticity in an ISI-dependent, non-linear form that are compatible with changes in synaptic plasticity. In addition, we showed that QPS interventions could interact in a metaplastic manner such that priming over M1 using QPS at short ISIs, which did not induce any plastic changes by itself, occluded subsequent LTP-like plasticity, whereas priming using QPS with long ISIs tended to do the reverse and increased the probability that facilitatory effects would be produced by a subsequent period of stimulation. The data support a BCM-like model of priming that shifts the crossover point at which the synaptic plasticity reverses from LTD to LTP. We proposed that such a broad range of after-effects produced by QPS facilitates detailed examinations of metaplasticity theories in humans (Hamada *et al.* 2008*a*). In the present study, we evaluated how LTD-like and LTP-like QPS-induced plasticity was altered by a preceding period of priming stimulation over SMA to understand metaplastic interplay between SMA and M1.

Methods

Subjects

Subjects were nine healthy volunteers (one woman, eight men; 27–45 years old, mean ± S.D., 34.5 ± 6.7 years) who gave their written informed consent to participate in the experiments. No subjects had neurological, psychiatric or other medical problems, or had any contraindication to TMS (Wassermann, 1998). All were right-handed according to the Oldfield handedness inventory (Oldfield, 1971). The protocol was approved by the Ethics Committee of the University of Tokyo and was carried out in accordance with the ethical standards of the *Declaration of Helsinki*. The procedures are in compliance with *The Journal of Physiology*'s guidelines for experimentation on humans (Drummond, 2009).

Recordings

Subjects were seated on a comfortable chair. The electromyogram (EMG) activity was recorded from the right first dorsal interosseous muscle (FDI) and the right tibialis anterior muscle (TA) using a belly-tendon arrangement. Responses were input to an amplifier (Biotop; GE Marquette Medical Systems, Japan) through filters set at 100 Hz and 3 kHz; they were then digitized and stored on a computer for later offline analyses (TMS bistim tester; Medical Try System, Japan).

Stimulation

Focal TMS was given using a hand-held figure-of-eight coil (9 cm external diameter at each wing; The Magstim Co. Ltd, Whitland, Dyfed, UK). Single monophasic TMS pulses were delivered by a magnetic stimulator (Magstim 200; The Magstim Co. Ltd). Quadripulse stimuli were delivered by four magnetic stimulators (Magstim 200²; The Magstim Co. Ltd) connected with a specially designed

DOI: 10.1113/jphysiol.2009.179101

combining module (The Magstim Co. Ltd). This device combines the outputs from four stimulators to allow a train of four monophasic magnetic pulses to be delivered through a single coil.

The optimal site for eliciting MEPs from the right FDI muscle (i.e. hot spot for FDI) was determined before each experiment and considered to be the primary motor cortex for FDI muscle ($M1_{FDI}$). A figure-of-eight coil was placed tangentially over the scalp with the handle pointing backwards at about 45 deg laterally. We stimulated several positions in 1 cm increments in the anterio-posterior and medio-lateral direction from each other using the same intensity and determined $M1_{FDI}$ as the site at which the largest responses were elicited. This position was marked with a blue pen on the scalp for repositioning the coil. The resting motor threshold for FDI (RMT_{FDI}) was defined as the lowest intensity that evoked a response of at least 50 μV in the relaxed FDI in at least 5 of 10 consecutive trials (Rossini *et al.* 1994). The active motor threshold for FDI (AMT_{FDI}) was defined as the lowest intensity that evoked a small response (>100 μV) when the subjects maintained a slight contraction of the right FDI (~10% of the maximum voluntary contraction), as observed using an oscilloscope monitor, in more than 5 of 10 consecutive trials. The stimulus intensity was changed in steps of 1% of the maximum stimulator output (MSO).

SMA stimulation was given with a coil centred at a point 3 cm anterior to the optimal site for eliciting MEPs in the right TA muscle (i.e. hot spot for TA) according to previous studies (Hikosaka *et al.* 1996; Lee *et al.* 1999; Terao *et al.* 2001; Matsunaga *et al.* 2005). The hot spot for TA was determined by moving the coil in 1 cm steps along the sagittal mid-line through the vertex (Cz) with the handle pointing to the right until we detected the position which evoked the largest MEP. This was considered to be the primary motor cortex for the TA muscle ($M1_{TA}$). We then used this position to determine the AMT for TA (AMT_{TA}). On average, the site of SMA stimulation (i.e. the point 3 cm anterior to $M1_{TA}$) was 2–3 cm anterior to Cz, in line with data from previous studies (Hikosaka *et al.* 1996; Lee *et al.* 1999; Matsunaga *et al.* 2005).

Measurement of motor cortical excitability

Motor cortical excitability was assessed by measuring the peak-to-peak amplitude of MEPs from the relaxed right FDI muscle elicited by single pulse TMS over the left $M1_{FDI}$ for all experiments. The stimulus intensity was adjusted to produce MEPs of about 0.5 mV in the right FDI muscle. During the experiments, EMG activity of the FDI was monitored with an oscilloscope monitor. Trials contaminated with voluntary EMG activities were discarded from analyses.

Quadripulse stimulation

The QPS protocol consisted of trains of TMS pulses with an inter-train interval (ITI) of 5 s (i.e. 0.2 Hz). Each train consisted of four magnetic pulses separated by inter-stimulus intervals (ISI) of 1.5, 5, 10, 30, 50 or 100 ms. These conditioning types were designated as QPS-1.5 ms to QPS-100 ms, respectively.

Experiment 1: Effects of SMA priming on subsequent QPS-induced plasticity

Six of nine subjects were enrolled. The experimental sessions were separated by 1 week or longer in the same subject. The order of the experiments was randomized and balanced among subjects.

Experiment 1a: QPS-induced plasticity without priming over SMA (Fig. 1). To investigate QPS-induced plasticity without any priming, conditioning stimulation was applied over the left $M1_{FDI}$ using QPS at various ISIs (QPS-1.5 ms, QPS-5 ms, QPS-10 ms, QPS-30 ms, QPS-50 ms and QPS-100ms) for 30 min (Fig. 1). The stimulus intensity of each pulse for QPS conditioning was set at 90% AMT_{FDI} (Hamada *et al.* 2008*a*). During the conditioning, no MEPs were observed.

Before QPS, 20 MEPs were obtained every 14.5–15.5 s using single-pulse TMS at a fixed intensity. The stimulus intensity was adjusted to produce MEPs of about 0.5 mV in the right FDI muscle at baseline (B1 in Fig. 1); the intensity was kept constant throughout the same experiment. After QPS conditioning, MEPs were measured every 5 min for 30 min. At each time point of the measurements, MEPs were collected in the same manner as baseline measurements.

Experiment 1b: QPS-induced plasticity with QPS-5 ms priming over SMA (Fig. 1). Priming stimulation was applied over SMA using QPS-5 ms for 10 min (i.e. four pulses at an ISI of 5 ms with an ITI of 5 s for 10 min). Importantly, priming over SMA using QPS-5 ms for 10 min induces no substantial effects on MEP sizes (see Results). The aim of the experiment was to test whether this priming stimulation would have effects on subsequent QPS-induced plasticity according to previous animal studies, which showed that prior induction of LTP is not prerequisite for metaplasticity (Abraham & Tate, 1997; Abraham, 2008). The stimulus intensity of each pulse for priming was set at 90% AMT_{TA}, which was identical to about 130% AMT_{FDI} (i.e. 90% RMT_{FDI}) (Table 1). The stimulus intensity used for priming over SMA was calculated relative to AMT_{TA} in order to secure effective stimulation of SMA, given that its depth is almost the same as that of the M1 for foot muscles in the interhemispheric fissure. Additionally, 130% AMT of hand muscle over SMA has been considered not to spread to the PMd or M1 (Matsunaga *et al.* 2005).

Subsequent conditioning was applied over the left $M1_{FDI}$ using QPS at various ISIs (QPS-1.5 ms, QPS-5 ms, QPS-10 ms, QPS-30 ms, QPS-50 ms and QPS-100ms) for 30 min (i.e. 360 trains, 1440 pulses in total) (Fig. 1). The stimulus intensity of each pulse for this subsequent conditioning was set at 90% AMT_{FDI}.

Before the priming stimulation (B0 in Fig. 1), 20 MEPs were collected every 14.5–15.5 s using single-pulse TMS at a fixed intensity, which was adjusted to elicit MEPs of about 0.5 mV in the right FDI muscle at B0 and kept constant throughout the experiment. After priming over SMA, 20 MEPs were again obtained in the same manner as measurements at B0 (B1 in Fig. 1). Following this measurement at B1 (i.e. immediately after priming), QPS conditioning of various types over the left $M1_{FDI}$ was performed. After each QPS, MEPs were measured every 5 min for 30 min (Fig. 1).

Experiment 1c: QPS-induced plasticity with QPS-50 ms priming over SMA (Fig. 1). QPS-50 ms for 10 min (i.e. four pulses at an ISI of 50 ms with an ITI of 5 s for 10 min) was selected as another priming stimulation over SMA to reveal the opposite priming effects to QPS-5 ms priming. The stimulus intensity for each pulse was set at 90% AMT_{TA}. Subsequent conditioning types after QPS-50 ms priming over SMA were QPS-5 ms, QPS-10 ms, QPS-30 ms and QPS-100 ms over the left $M1_{FDI}$ for 30 min. We have previously shown that QPS-50 ms priming over M1 produced substantial changes in subsequent QPS-induced plasticity at ISIs of

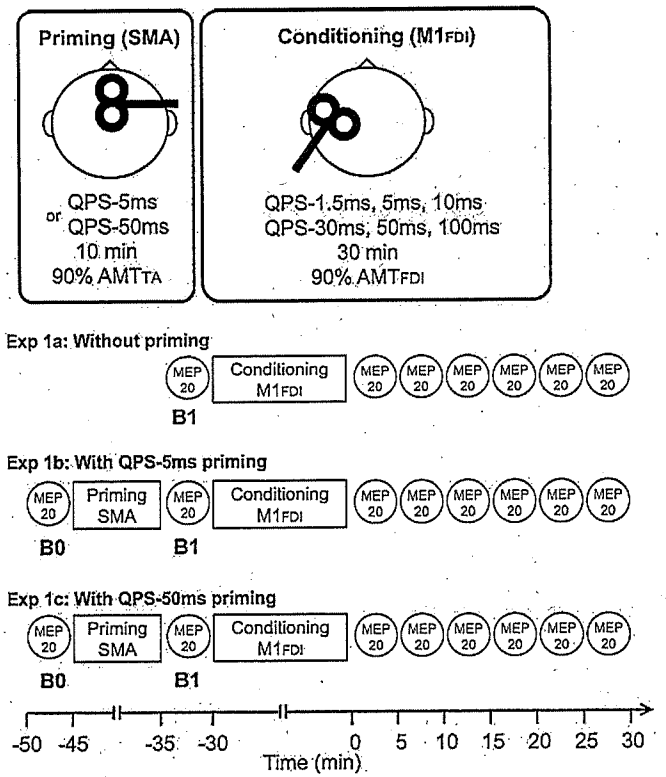

Figure 1. Timelines of experiments
(See Methods.)

Table 1. Physiological parameters (mean ± S.D.)

	RMT_{FDI}	AMT_{FDI}	AMT_{TA}	Stimulus intensify for SMA priming (relative to RMT_{FDI})	MEP size (mV), right FDI	
Experiment 1a: Without priming		Baseline (B1)				B1
QPS-1.5 ms	57.1 ± 9.8%	40.8 ± 6.9%	–	–	–	0.46 ± 0.11
QPS-5 ms	58.5 ± 9.5%	43.6 ± 5.1%	–	–	–	0.51 ± 0.13
QPS-10 ms	61.8 ± 10.9%	41.0 ± 6.6%	–	–	–	0.48 ± 0.16
QPS-30 ms	61.2 ± 11.6%	40.6 ± 5.8%	–	–	–	0.49 ± 0.09
QPS-50 ms	60.5 ± 14.1%	42.6 ± 5.4%	–	–	–	0.51 ± 0.18
QPS-100 ms	60.1 ± 12.1%	40.8 ± 5.8%	–	–	–	0.55 ± 0.06
Experiment 1b: With QPS-5 ms priming over SMA		Baseline (B1)		Mean ± S.D. (range)	B0	B1
QPS-1.5 ms	61.8 ± 9.2%	40.3 ± 1.9%	60.2 ± 8.0%	89 ± 8% (76–98%)	0.51 ± 0.09	0.49 ± 0.14
QPS-5 ms	59.8 ± 6.9%	42.8 ± 5.0%	60.8 ± 8.5%	92 ± 5% (85–97%)	0.43 ± 0.11	0.47 ± 0.28
QPS-10 ms	60.0 ± 9.7%	42.0 ± 4.9%	61.1 ± 10.0%	93 ± 4% (87–99%)	0.48 ± 0.18	0.54 ± 0.14
QPS-30 ms	58.3 ± 8.5%	41.7 ± 5.4%	60.8 ± 10.0%	95 ± 6% (86–100%)	0.51 ± 0.14	0.55 ± 0.18
QPS-50 ms	61.8 ± 7.6%	41.0 ± 5.1%	63.6 ± 8.1%	93 ± 5% (85–98%)	0.53 ± 0.21	0.53 ± 0.20
QPS-100 ms	60.8 ± 8.7%	40.3 ± 5.0%	61.5 ± 7.6%	92 ± 4% (86–96%)	0.53 ± 0.18	0.59 ± 0.21
Experiment 1c: With QPS-50 ms priming over SMA		Baseline (B1)			B0	B1
QPS-5 ms	61.6 ± 9.4%	41.6 ± 5.3%	62.6 ± 9.3%	94 ± 3% (91–98%)	0.50 ± 0.09	0.52 ± 0.08
QPS-10 ms	60.6 ± 9.1%	43.8 ± 5.9%	63.5 ± 9.6%	95 ± 2% (92–98%)	0.57 ± 0.11	0.53 ± 0.21
QPS-30 ms	58.1 ± 9.9%	42.1 ± 4.8%	62.2 ± 11.4%	95 ± 5% (88–100%)	0.53 ± 0.09	0.48 ± 0.04
QPS-100 ms	60.5 ± 10.1%	42.0 ± 6.4%	65.2 ± 11.7%	97 ± 3% (93–100%)	0.52 ± 0.12	0.49 ± 0.16
Experiment 2		Baseline (B0)			B0	B1
Sham with priming	61.8 ± 13.7%	40.8 ± 7.8%	61.5 ± 7.2%	93 ± 4% (88–100%)	0.46 ± 0.06	0.51 ± 0.14
QPS-10 ms with sham priming	58.3 ± 7.4%	40.5 ± 7.4%	–	–	0.47 ± 0.12	0.48 ± 0.18
Experiment 3		Baseline			Baseline	Post 1	Post 2
QPS-5 ms priming	60.6 ± 11.0%	42.0 ± 8.2%	66.0 ± 7.7%	95 ± 4% (88–100%)	0.52 ± 0.24	0.54 ± 0.27	0.49 ± 0.26
QPS-50 ms priming	59.7 ± 10.1%	41.5 ± 9.8%	66.4 ± 8.3%	95 ± 5% (88–100%)	0.48 ± 0.14	0.53 ± 0.19	0.55 ± 0.11
Experiment 4					ISI 3 ms	ISI 6 ms	
	57.9 ± 9.6%	43.3 ± 7.8%	62.6 ± 9.4%	–	0.59 ± 0.23	0.58 ± 0.27	

10, 30 and 100 ms (Hamada *et al.* 2008*a*). Since it would be of value to compare those results and SMA priming effects in the present study to understand the difference in priming stimulation site (i.e. M1 *versus* SMA), we selected the four ISIs used in the previous paper for Experiment 1c. The stimulus intensity of each pulse of QPS conditioning was set at 90% AMT_{FDI}. MEP measurements were exactly the same as those of Experiment 1b.

Experiment 2: Control experiments

In the first control experiment (Fig. 6*A*), priming stimulation using QPS-5 ms over SMA for 10 min was followed by sham conditioning stimulation (i.e. sham with priming) to examine whether the priming alone affects motor cortical excitability. In the second control experiment (Fig. 6*B*), sham priming stimulation was followed by QPS-10 ms over M1 to confirm that sham priming did not affect the QPS-induced plastic changes (QPS-10 ms with sham priming). QPS-10 ms was chosen as conditioning because this protocol induced mild facilitatory after-effects (see Results) which we thought might make it more susceptible to any bidirectional effects of sham priming.

The sham stimulation procedure used for these control experiments was identical to those described in our previous reports (Okabe *et al.* 2003; Hamada *et al.* 2008*b*). In brief, four electric pulses (each electric pulse was of 0.2 ms duration with intensity of twice the sensory threshold) were given to the scalp at 0.2 Hz at an ISI of 10 ms for sham conditioning (first control experiment) and at 5 ms for sham priming (second control experiment) with a conventional electric peripheral nerve stimulator to mimic the skin sensation of TMS. Electric pulses were applied through the electrodes placed over the left $M1_{FDI}$ or SMA and the vertex. A coil, which was disconnected from the stimulator, was placed over the left $M1_{FDI}$ or SMA to mimic real TMS. Another coil, which was connected to a combining module with four stimulators, was held off the scalp but placed near the subject. This coil was discharged simultaneously with the scalp electrical stimulation to produce a similar sound to that associated with real QPS.

Experiment 3: Effects of priming over SMA on intracortical circuits of M1

Nine subjects participated in this experiment. To explore the effects of SMA priming alone on either excitatory or inhibitory circuits of M1, short-interval intracortical inhibition (SICI), intracortical facilitation (ICF) (Kujirai *et al.* 1993), short-interval intracortical facilitation (SICF) (Tokimura *et al.* 1996; Ziemann *et al.* 1998; Hanajima *et al.* 2002), and long-interval intracortical inhibition (LICI) (Valls-Sole *et al.* 1992; Wassermann *et al.* 1996) were measured using the paired-pulse technique before and after QPS-5 ms or QPS-50 ms priming over SMA (i.e. four pulses at an ISI of 5 ms or 50 ms with an ITI of 5 s for 10 min; the stimulus intensity of each pulse, 90% AMT_{TA}).

SICI was examined at an ISI of 3 ms using a conditioning stimulus (CS) intensity of 80% AMT_{FDI}. ICF was measured at an ISI of 10 ms with a CS intensity of 90% AMT_{FDI}. SICF was measured at an ISI of 1.5 ms. The intensity of the second stimulus (S2) was set at 10% below AMT_{FDI}. LICI was measured at an ISI of 100 ms with a CS intensity of 110% RMT_{FDI}. The intensity of the test stimulus (TS) (i.e. the first stimulus (S1) for SICF) was adjusted to elicit MEPs of 0.4–0.5 mV from relaxed FDI at baseline. Twelve trials were recorded for each condition and randomly intermixed with 18 trials of TS alone with an ITI of 5.5–6.5 s (about 6 min in total). The SICI, ICF, SICF and LICI were all studied simultaneously in one session using the four magnetic stimulators (i.e. three stimulators produced the different CS and the other one gave TS). Measurements of these values were performed in blocks immediately before (baseline) and just after QPS-5 ms priming (post 1) as well as 20 to 26 min (post 2). Conditioning intensities and test intensity were not changed after the priming because the test MEP sizes were not altered by SMA priming (see Results and Table 1).

Experiment 4: Supplementary experiments

The aim of these experiments was to test whether the conditioning stimulus over SMA spreads to M1 or PMd (Experiment 4a), or whether it exerts a direct effect on the spinal motor neurons (Experiment 4b). Eight subjects participated in this series of experiments.

Experiment 4a: Effects of a conditioning stimulus over SMA on MEP. We investigated whether the stimulus over SMA spreads to other cortical areas using a paired-pulse technique. The test response in the right relaxed FDI elicited by single pulse TMS over the left $M1_{FDI}$ was conditioned by single pulse TMS over SMA at an ISI of 3 ms or 6 ms. The intensity of the TS was adjusted to elicit MEPs of about 0.5 mV in the relaxed FDI when given alone. The stimulus intensities for conditioning over SMA were set at 70, 90 and 110% AMT_{TA}. At each ISI (i.e. 3 or 6 ms), 12 trials were recorded for each condition (70, 90 and 110% AMT_{TA}) and randomly intermixed with 18 trials of TS alone with an ITI of 5.5–6.5 s in a single block. Thus, two blocks of measurements at each ISI were performed. The order of blocks was randomized. As the inhibitory interneurons of the $M1_{FDI}$ might have a lower threshold than the intrinsic I-wave circuits (Reis *et al.* 2008), we argued that, if the current over SMA spread to the $M1_{FDI}$, then some inhibitory effects on the test response would be observed at an ISI of 3 ms in a conditioning intensity-dependent manner. Indeed, it is known that conditioning over the PMd at an ISI of 6 ms has either inhibitory or facilitatory effects on MEP sizes depending on the conditioning intensity (Civardi *et al.* 2001). Thus, we argued that, if the current over SMA spread to PMd, then some inhibitory or facilitatory effects on the test response would be observed in an intensity-dependent manner.

Experiment 4b: Effects of a stimulus over SMA on MEP in active condition. To test whether the current over SMA spreads to the $M1_{FDI}$ directly and whether direct stimulation of SMA activates some neurons in SMA projecting to the spinal motor neurons directly (Dum & Strick, 1991, 1996), single pulse TMS was applied over SMA during contraction of the right FDI muscle (20% maximum voluntary contraction). If the current over SMA spread to $M1_{FDI}$ directly or if the current stimulated some SMA neurons enough to produce any descending volley, then small MEPs would be elicited during voluntary contraction in an intensity-dependent manner. Ten stimuli were applied every 5 s at an intensity of 100% AMT_{TA}. The stimulus intensity was then increased by 10% of AMT_{TA} and another 10 stimuli were applied. This process was repeated until the intensity reached 190% AMT_{TA} or 100% MSO.

Data analyses

Experiment 1a. The after-effects of different conditioning types were analysed with absolute MEP amplitudes using two-way repeated-measures analysis of variance (ANOVA) (within-subject factors, CONDITION (QPS-1.5 ms, QPS-5 ms, ···, QPS-100ms), and TIME (B1 and following six time points)). If the factors CONDITION and TIME showed a significant interaction, *post hoc* paired *t* tests (two-tailed) with Bonferroni's corrections for multiple comparisons were used for further analyses. The Greenhouse–Geisser correction was used if necessary to correct for non-sphericity; *P* values less than 0.05 were considered significant.

Experiment 1b and 1c. Absolute values of MEPs at B0 and B1 (Fig. 1) were compared using paired *t* tests in each experiment. To evaluate the priming effects on subsequent QPS-induced plasticity, the absolute amplitudes of MEPs collected in Experiment 1a (i.e. without priming) and Experiment 1b (i.e. with QPS-5 ms priming over the SMA) or Experiment 1c (i.e. with QPS-50 ms priming over the SMA) were entered in three-way repeated-measures ANOVA with PRIMING (with and without priming), CONDITION ((QPS-1.5 ms, QPS-5 ms, ···, and QPS-100ms) for Experiment 1b, and (QPS-5 ms, QPS-10 ms, QPS-30 ms and QPS-100ms) for Experiment 1c), and TIME (B1, and following six time points) as within-subject factors to match the measurement time points relative to QPS conditioning among experiments. Additionally, it might be valid to evaluate the effect of priming stimulation on subsequent QPS-induced plasticity using these values because the absolute amplitudes obtained at B0 and B1 were not significantly different (see Results). If the factors PRIMING, CONDITION and TIME showed a significant interaction, *post hoc* paired *t* tests (two-tailed) with Bonferroni's corrections for multiple comparisons were used.

Experiment 2. The time course of after-effects for the first control experiment (i.e. sham conditioning with real priming) on absolute MEP sizes was analysed using one-way repeated measures ANOVA (within-subject factor, TIME (B1 and following six points)). For the second control experiment, the after-effects of QPS-10 ms with sham priming were compared with those of QPS-10 ms without priming using two-way repeated-measures ANOVA (within-subject factors, CONDITION (QPS-10 ms with sham priming, QPS-10 ms without priming) and TIME (B1 and following six points)).

Experiment 3. The ratio of the mean amplitude of the conditioned response to that of the control response was calculated for each condition in each subject. These individual mean ratios were then averaged to give a grand mean ratio. The time course of after-effects was analysed using three-way repeated measures ANOVA (within-subject factors, PRIMING (QPS-5 ms and QPS-50ms), BISTIM (SICI, ICF, SICF and LICI) and TIME (baseline, post 1 and post 2)). If the factors PRIMING, BISTIM and TIME showed a significant interaction, Dunnett's *post hoc* test in each condition was used for further analyses.

Experiment 4a. The ratio of the mean amplitude of the conditioned response to that of the control response was calculated for each condition in each subject. These individual mean ratios were then averaged to give a grand mean ratio. The ratios were entered in one-way repeated measures ANOVA (within-subject factor, INTENSITY of conditioning stimulation). Paired *t* tests (two-tailed) were used for further analyses.

Data were analysed with the commercialized software (SPSS version 17.0 for Windows; SPSS Inc.). All figures depict the group data.

Results

None of the subjects reported any adverse effects during or after any of the experiments. Baseline physiological data did not differ significantly among different experiments (Table 1). The stimulus intensities for SMA priming were all below RMT_{FDI} (Table 1).

Experiment 1: Effects of SMA priming on subsequent QPS-induced plasticity

Experiment 1a: QPS-induced plasticity without priming over SMA. In line with our previous report (Hamada *et al.* 2008*a*), QPS at short ISIs (QPS-1.5 ms, QPS-5 ms and QPS-10ms) produced an increase in the MEP amplitude, whereas QPS at long ISIs (QPS-30 ms, QPS-50 ms and QPS-100ms) suppressed MEPs (Fig. 2*A*). Two-way repeated measures ANOVA revealed a significant CONDITION (QPS-1.5 ms, QPS-5 ms, ···, and QPS-100ms) × TIME interaction ($F_{(2.941,14.705)} = 4.384$, $P < 0.001$). Figure 2*B* presents the MEP amplitude normalized to the baseline MEP at 30 min after QPS as a function of the reciprocal of the ISI used in each QPS burst. There was a non-linear relation between MEP excitability changes and ISI indicating the presence of threshold for inducing LTP-like plasticity. *Post hoc* analysis revealed that QPS-1.5 ms, QPS-5 ms and QPS-50ms were significantly different from QPS-30 ms.

Experiment1b: QPS-induced plasticity with QPS-5 ms priming over SMA. Figure 3 shows the time courses

of MEP amplitude following QPS at various ISIs with and without QPS-5 ms priming over SMA. No difference was found in MEP amplitudes at B0 and B1 in any conditions (paired *t* test, $P > 0.5$). Although SMA priming with QPS-5 ms did not occlude MEP facilitation by QPS-1.5 ms, it produced lasting MEP suppression after QPS-5 ms, QPS-10 ms and QPS-30 ms (Fig. 3*B–D*). By contrast, MEP suppression induced by QPS-50 ms and QPS-100 ms was not enhanced, but its duration was shortened by SMA priming (Fig. 3*E* and *F*). Three-way repeated measures ANOVA revealed a significant PRIMING × CONDITION × TIME interaction ($F_{(3.464,17.319)} = 3.826$, $P = 0.025$). *Post hoc* paired *t* tests revealed a significant effect of SMA priming on the after-effects of QPS-5 ms, QPS-10 ms, QPS-30 ms, QPS-50 ms and QPS-100 ms (Fig. 3*A–F*).

Experiment 1c: QPS-induced plasticity with QPS-50 ms priming over SMA. Figure 4 shows the change in MEP amplitude following QPS at various ISIs with and without QPS-50 ms priming over SMA. No difference in MEP amplitude was found at B0 and B1 in any conditions (paired *t* test, $P > 0.5$). QPS-50 ms priming over SMA did not enhance MEP facilitation by QPS-5 ms. It produced slight enhancement of MEP facilitation by QPS-10 ms (Fig. 4*A* and *B*). In contrast, transient MEP suppression induced by QPS-30 ms turned to facilitation after SMA priming, but there was no change in the after-effects of QPS-100 ms (Fig. 4*C* and *D*). Three-way repeated measures ANOVA revealed a significant PRIMING × CONDITION interaction ($F_{(2.593,9.948)} = 5.612$, $P = 0.023$), but revealed no significant PRIMING × CONDITION × TIME interaction ($F_{(3.363,16.810)} = 3.079$, $P = 0.051$). The results reveal that priming stimulation affected subsequent QPS-induced plasticity, irrespective of the time after QPS conditioning. *Post hoc* paired *t* tests revealed a significant effect of SMA priming with QPS-50 ms on the after-effects of QPS-5 ms and QPS-30 ms (Fig. 4*A* and *C*).

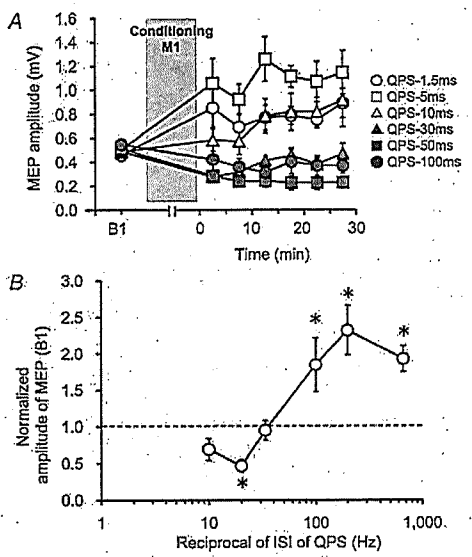

Figure 2. QPS-induced plasticity without priming over SMA
A, time courses of MEP amplitude following QPS at various ISIs without priming (mean ± S.E.M.). *B*, stimulus–response function of QPS-induced plasticity. Normalized amplitudes of MEP measured at 30 min after QPS as a function of the reciprocal of ISI of QPS: mean (± S.E.M.) of baseline. Note that the *x*-axis is logarithmic. Asterisks denote significant difference from QPS-30 ms (*$P < 0.05$).

Stimulus–response function with priming over SMA. The normalized MEP amplitudes at 30 min post conditioning are plotted as a function of the reciprocal of the ISI used in each QPS with and without priming over SMA (Fig. 5). The crossover point from MEP suppression to facilitation appears to shift in either direction along the *x*-axis according to which priming stimulation was employed. *Post hoc* analysis revealed that QPS-5 ms priming over SMA significantly reduced MEP sizes after QPS-5 ms, QPS-10 ms and QPS-30 ms, but occluded MEP suppression by QPS-50 ms. QPS-50 ms priming over SMA inhibited MEP sizes after QPS-5 ms, whereas it facilitated MEP sizes after QPS-30 ms (Fig. 5).

Experiment 2: Control experiments

First, the after-effects of sham conditioning with real priming were monitored to examine whether priming alone (i.e. QPS-5 ms over SMA for 10 min) affects motor cortical excitability. Figure 6*A* shows the time course of the MEP amplitude following sham conditioning with real priming. No difference was found in MEP amplitudes at B0 and B1 (paired *t* test, $P > 0.5$). Sham conditioning with real priming did not change the MEP amplitude for at least 30 min after conditioning (one-way repeated measures ANOVA: effect of TIME, $F_{(6,30)} = 0.410$, $P = 0.866$). Second, the after-effect of real conditioning (QPS-10ms) with sham priming was compared to that of real conditioning without priming to confirm that sham priming did not affect motor cortical plasticity induced by real conditioning. Figure 6*B* shows the absolute amplitude of MEPs following real conditioning (QPS-10ms) without priming and with sham priming. No difference was found between MEPs at B0 and B1 (paired *t* test, $P > 0.5$). Furthermore, MEP amplitudes following QPS-10 ms with sham priming

were not different from those without priming (two-way repeated measures ANOVA: effect of CONDITION (QPS-10 ms with sham priming, QPS-10 ms without priming), $F_{(1,5)} = 0.095$, $P = 0.770$; CONDITION × TIME interaction, $F_{(6,30)} = 0.410$, $P = 0.866$).

Experiment 3: Effects of priming over SMA on intracortical circuits of M1

Figure 7 shows the effects of priming over SMA on SICI, ICF, SICF and LICI. Three-way repeated measures ANOVA revealed significant PRIMING × BISTIM × TIME interaction ($F_{(6,48)} = 2.498$, $P = 0.035$). *Post hoc* tests revealed that only SICF was modulated after SMA priming; the effects on SICF were transient, being significant only at post 1 (Fig. 7*A* and *B*).

Experiment 4: Supplementary experiments

Experiment 4a: Effects of a conditioning stimulus over the SMA on MEP. Using the paired-pulse technique at an ISI of 3 ms, we investigated whether the stimulus over SMA spreads to $M1_{FDI}$. Figure 8*A* shows the changes of conditioned MEP relative to the unconditioned MEP in each block using three different conditioning intensities. One-way repeated measures ANOVA revealed a significant main effect of INTENSITY ($F_{(2,14)} = 3.904$, $P = 0.045$). *Post hoc* paired *t* tests revealed that the test MEPs were significantly inhibited by conditioning stimulus at 110% AMT_{TA} ($t = 2.39$, $P = 0.048$), whereas no significant inhibition was found at 70% or 90% AMT_{TA}.

Figure 8*B* shows the changes of conditioned MEP relative to the unconditioned MEP using the paired-pulse technique at an ISI of 6 ms. No significant effect of conditioning intensity over SMA at an ISI of 6 ms was found (one-way repeated measures ANOVA: effect of INTENSITY, $F_{(2,14)} = 0.679$, $P = 0.523$).

Experiment 4b: effects of a stimulus over the SMA on MEP in active condition. To test whether the current induced by TMS over the SMA directly spreads to the $M1_{FDI}$, single pulse TMS was applied over SMA during contraction of the right FDI muscle (20% maximum). Although the stimulus intensity reached 190% AMT_{TA} or 100% MSO, no MEPs were recorded in any condition.

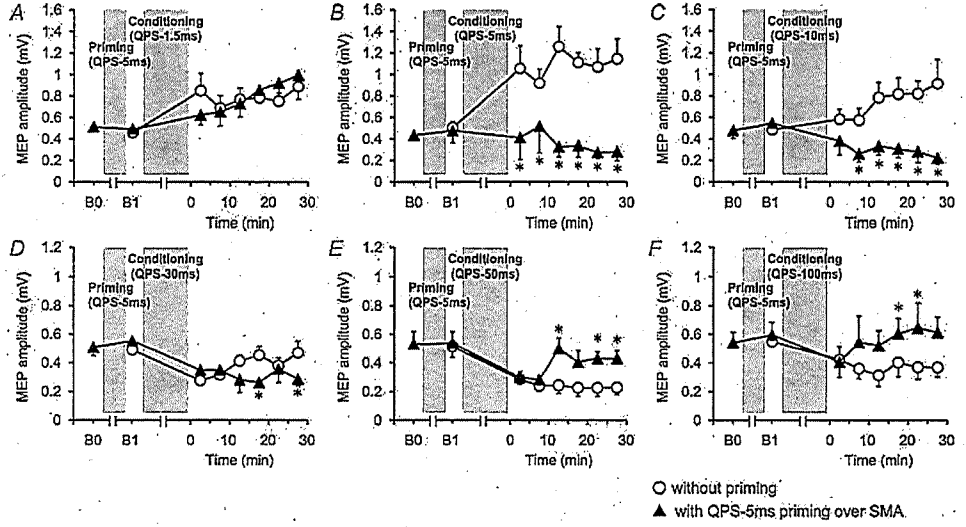

Figure 3. Effects of QPS-5 ms priming over SMA on QPS-induced plasticity
Time courses of MEP amplitude following QPS at various ISIs with (▲) and without (○) QPS-5 ms priming over SMA (mean ± S.E.M.). *A*, SMA priming did not change subsequent LTP-like plasticity induced by QPS-1.5 ms. *B* and *C*, priming reversed MEP sizes induced by QPS-5 ms (*B*) or QPS-10 ms (*C*). *D*, priming enhanced suppression of MEP by QPS-30 ms. *E* and *F*, MEP suppression induced by QPS-50 ms (*E*) and QPS-100 ms (*F*) were not enhanced, but shortened with SMA priming. Asterisks denote significant difference of MEP sizes with priming from those without priming at each time point ($P < 0.05$ by *post hoc* paired *t* tests).

Discussion

We showed that LTD-like and LTP-like QPS-induced plasticity was altered by a preceding period of priming stimulation over SMA. QPS at short ISIs produced an increase in the MEP amplitude, whereas QPS at long ISIs suppressed MEPs (Experiment 1a, Fig. 2*A*). QPS-5 ms priming over SMA occluded MEP facilitation after QPS-5 ms and QPS-10 ms. Furthermore, it enhanced suppression of MEP after QPS-30 ms, but occluded MEP suppression by QPS-50 ms (Experiments 1b, Fig. 5). By contrast, QPS-50 ms priming over SMA inhibited MEP sizes after QPS-5 ms, whereas it facilitated MEP sizes after QPS-30 ms (Experiments 1c, Fig. 5). QPS-5 ms or QPS-50 ms priming over SMA did not change MEP sizes, SICI, ICF and LICI but altered SICF; QPS-5 ms priming enhanced SICF, whereas QPS-50 ms priming erased SICF (Experiment 3, Fig. 7). Finally, a single conditioning TMS over SMA at 110% AMT_{TA} with an ISI of 3 ms significantly inhibited test MEP sizes, whereas no effect was found at a conditioning intensity lower than 110% AMT_{TA}. In addition, no significant effects were found at any conditioning intensity using an ISI of 6 ms (Experiment 4, Fig. 8). We will argue that the present findings provide strong support for the hypothesis that priming over the SMA transiently altered the synaptic efficiencies of excitatory circuits within M1, and that such prior history of neuronal activity alters subsequent LTD-like and LTP-like QPS-induced plasticity through the metaplastic interplay between SMA and M1.

Effects of TMS over SMA

Given that there is now good evidence that TMS can stimulate SMA neurons (Civardi *et al.* 2001; Terao *et al.* 2001; Serrien *et al.* 2002; Verwey *et al.* 2002; Matsunaga *et al.* 2005; Hamada *et al.* 2008*b*), our results are compatible with the idea that rTMS can produce lasting changes in the excitability of these circuits. We argue that such mechanisms underpin the present findings, although we cannot be completely certain about the precise site of our SMA stimulus. According to previous studies, the optimal site of SMA stimulation has been shown to be between 2 and 4 cm anterior to Cz (Terao *et al.* 2001; Serrien *et al.* 2002; Verwey *et al.* 2002); neuroimaging methods also locate the hand area of the SMA proper some 2 to 3 cm anterior to Cz (Hikosaka *et al.* 1996; Lee *et al.* 1999). It is thereby conceivable that our TMS stimulus mainly activates SMA neurons.

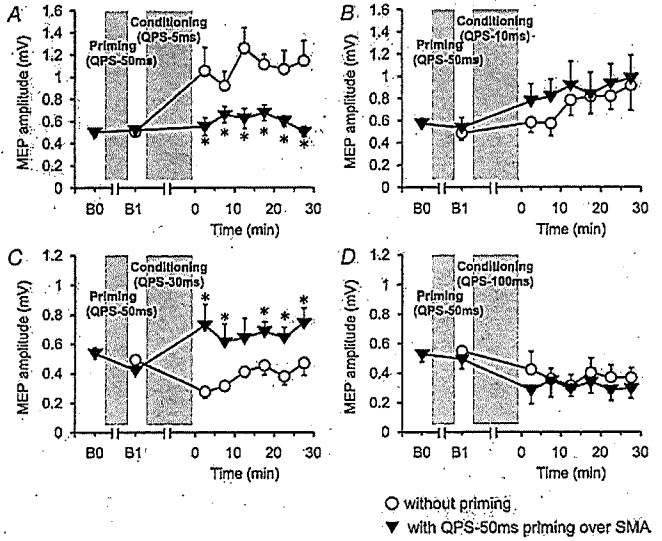

Figure 4. Effects of QPS-50 ms priming over SMA on QPS-induced plasticity
Time courses of MEP amplitude following QPS at various ISIs with (▼) and without (○) QPS-50 ms priming over SMA (mean ± S.E.M.). *A*, SMA priming occluded subsequent LTP-like plasticity induced by QPS-5 ms. *B*, priming did not change plasticity induced by QPS-10 ms. *C*, priming reversed suppression of MEP by QPS-30 ms. *D*, MEP suppression induced by QPS-100 ms was not altered with SMA priming. Asterisks denote significant difference of MEP sizes with priming from those without priming at each time point ($P < 0.05$ by *post hoc* paired *t* tests).

A second question is whether currents induced by stimulation over SMA spread to other motor-related areas. The data suggest that this was unlikely with the intensities of stimulation that we used. Experiment 4a showed that a conditioning pulse over SMA at 110% AMT_{TA} with an ISI of 3 ms significantly inhibited test MEP sizes, which corresponds to the timing of SICI (Kujirai *et al.* 1993), whereas no effect was found at a conditioning intensity of either 70% AMT_{TA} or 90% AMT_{TA}. These findings suggest that the current induced by placing the coil over SMA spreads to $M1_{FDI}$ only when the stimulus intensity is higher than 110% AMT_{TA} in line with a preceding report (Matsunaga *et al.* 2005). In addition, no significant changes in the size of test responses were found at any conditioning intensity using an ISI of 6 ms, which corresponds to the optimal ISI to produce effects in the pathway from PMd to M1 (Civardi *et al.* 2001). Finally, Experiment 4b revealed that no MEPs were elicited during voluntary contraction with single pulse TMS over SMA at very high stimulus intensities up to 100% MSO, indicating no direct activation of excitatory interneurons or cortical output neurons within M1. We cannot completely exclude the possibility that various subliminally stimulated cortical areas including SMA, PMd, PMv, M1 and others regions were implicated in the effects of SMA priming. However, the present findings lead us to conjecture that the effects of priming over SMA can be mainly ascribed to stimulation of the cortex beneath the coil, namely SMA.

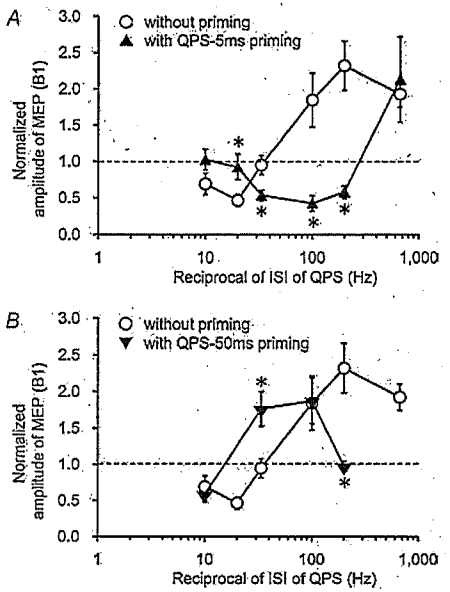

Figure 5. Priming-induced shifts in the stimulus–response function
The normalized amplitudes of MEP at 30 min post conditioning as a function of the reciprocal of ISI of QPS with and without priming over SMA (○). *A*, QPS-5 ms priming (▲). *B*, QPS-50 ms priming (▼). Note that the *x*-axis is logarithmic axis. **P* < 0.05 by *post hoc* paired *t* tests.

Effects of priming over SMA alone

We did not evaluate possible effects of sham priming on subsequent QPS-induced plasticity elicited by all kinds of QPS protocols used in the present paper. In Experiment 2, QPS-10 ms was chosen as a representative of all QPS protocols because it induced mild facilitatory after-effects rendering it more susceptible to possible effects of sham priming. In fact, two control experiments revealed that neither priming alone nor cutaneous sensation had any lasting effect on MEPs.

The results of Experiment 3 show that QPS-5 ms or QPS-50 ms priming over SMA did not change MEP sizes, SICI, ICF and LICI. Its only effect was a transient modulation of SICF, which did not persist as long as the priming effects on QPS. We cannot exclude the possibility that subtle changes in inhibitory circuits were missed because paired-pulse measurements addressing

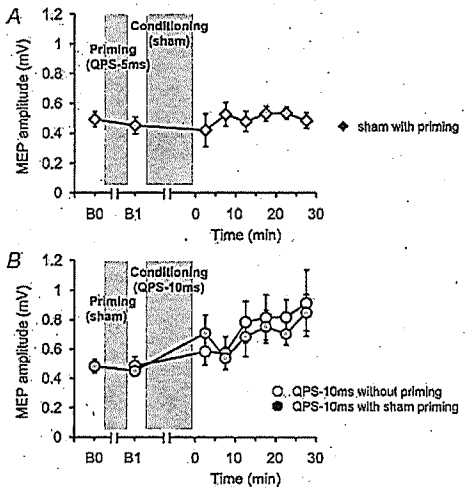

Figure 6. Control experiments
A, sham conditioning with real priming did not modify motor cortical excitability. *B*, the after-effects of QPS-10 ms without priming (open circles) were not different from those of QPS-10 ms with sham priming (grey circles).

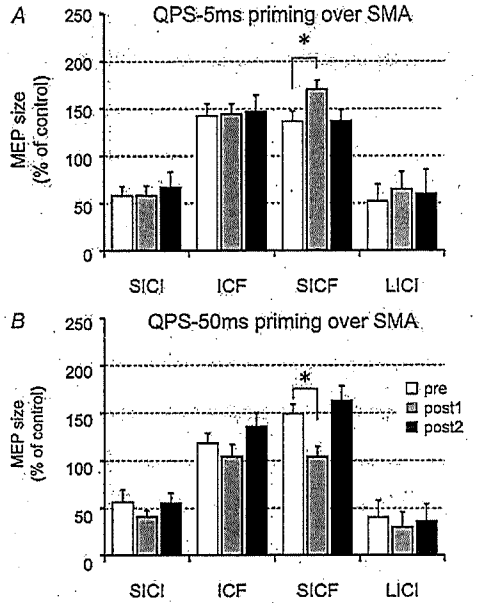

Figure 7. Effects of priming over SMA on intracortical circuits of M1
A, SICF was enhanced after QPS-5 ms. SICI, ICF nor LICI were altered by QPS-5 ms priming over SMA alone. *B*, SICF was suppressed after QPS-50 ms over SMA, whereas others were not altered. Baseline (white bars); post 1 (grey bars), 0–6 min after QPS; post 2 (black bars), 20–26 min after QPS over SMA. **P* < 0.05 by *post hoc* Dunnett's test.

intracortical excitability were assessed only at a single ISI with a single conditioning intensity. Nonetheless, the long period for measurements using various ISIs with multiple conditioning intensities might in turn miss the effects of priming owing to transient effects of priming on SICF.

The present results raise the question why such selective modulation of SICF was produced by SMA priming. Although this selectivity seems puzzling, it is not a unique observation since we have shown that QPS priming over M1 produced transient modulation of SICF without affecting MEP sizes, SICI, ICF and LICI (Hamada *et al.* 2008*a*). It has been also reported that selective modulation of SICI can be produced by low-intensity theta burst stimulation (TBS) without any changes in MEP (McAllister *et al.* 2009). Also, 5 Hz rTMS over PMd reduced paired-pulse excitability at an ISI of 7 ms without any changes in MEP amplitude (Rizzo *et al.* 2004). Thus, it is possible to modulate inhibitory or excitatory circuits selectively, which is not accompanied by lasting changes in MEP sizes under certain specified conditions.

What is the mechanism behind the modulation of SICF by SMA priming? At first, an interaction of I-wave inputs is thought to be the cause of SICF presumably by the summation of excitatory postsynaptic potentials (EPSPs) elicited by the first suprathreshold TMS stimulus with subliminal depolarization of interneurons that is produced by the second subthreshold TMS in cortical interneurons (Hanajima *et al.* 2002). Thus, modulation of SICF by SMA priming might therefore be consistent with the idea that SMA priming alters synaptic efficiency at which I-waves summate during paired-pulse TMS.

Then why are such changes in excitatory circuits of M1 produced by SMA priming? Matsunaga *et al.* (2005) proposed that there are at least two possible explanations for modulation of motor cortical excitability produced by rTMS over SMA. One possibility is that rTMS over SMA stimulates mainly cortico-cortical projections from SMA to M1 (Dum & Strick, 1991; Tokuno & Nambu, 2000; Nachev *et al.* 2008). The other is that rTMS over SMA alters local balance of excitability within SMA, leading to alteration of activity of cortico-cortical projections from

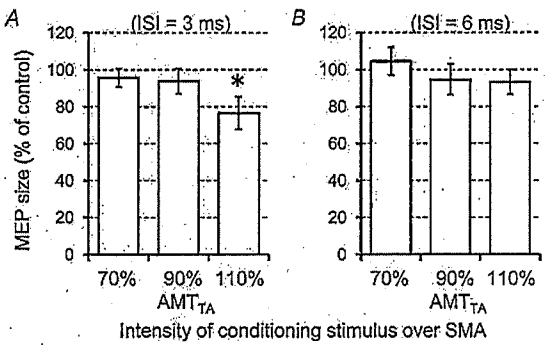

Figure 8. Effects of a conditioning stimulus over SMA on MEP
The test MEPs evoked by the left $M1_{FDI}$ was conditioned by stimulation of SMA at an ISI of 3 ms (*A*) or at an ISI of 6 ms (*B*). Asterisks denote a significant change relative to unconditioned response.

SMA to M1. They conclude that the latter might pertain to their findings since the intensity of stimulation was low (Matsunaga *et al.* 2005). The present study as with the previous study was not designed to test these hypotheses, thus we cannot comment on this issue further. Besides, it is also possible that functional modulation of basal ganglia via cortico-subcortical connections might contribute to the effects of priming over SMA (Inase *et al.* 1999; Kaneda *et al.* 2002; Akkal *et al.* 2007). Several studies also suggest that SMA proper sends direct projections to the spinal cord (Dum & Strick, 1991, 1996). Thus, SMA priming could produce some excitability changes in spinal motor neurons. However, it was impossible to evoke any MEPs during voluntary contraction of hand muscle using TMS over SMA at any intensities from 100% AMT_{TA} to 190% AMT_{TA} (i.e. 100% MSO), indicating that a higher intensity (above 100% MSO) is needed to stimulate neurons in SMA that project directly to the spinal cord. We cannot exclude the fact that repetitive stimulation of SMA with QPS, even at low intensities, might produce subthreshold temporal facilitation at spinal interneurons. In any case, we showed that QPS over SMA for 10 min produced bidirectional changes in SICF. Based on the fact that lasting motor cortical plasticity was induced by QPS over M1 for 30 min (Hamada *et al.* 2008*a*), the present result raises a new question as to whether QPS over SMA for 30 min produces plastic changes in bilateral M1. The issue should be addressed in future studies.

QPS-induced plasticity and synaptic plasticity

QPS is a newly developed protocol for inducing bidirectional (i.e. either facilitatory or inhibitory) motor cortical plasticity in humans (Hamada *et al.* 2007, 2008*a*). QPS at short intervals facilitated MEPs for more than 75 min, whereas QPS at long intervals suppressed MEPs for more than 75 min. The QPS-induced plasticity appears to be rather synapse-specific, as suggested by the following in the previous study (Hamada *et al.* 2008*a*); motor thresholds, which are dependent on ion channel conductivity and might reflect membrane excitability (Mavroudakis *et al.* 1994, 1997; Ziemann *et al.* 1996; Chen *et al.* 1997), were unchanged after QPS; SICI, which is considered to reflect γ-aminobutyric acid (GABA)-ergic inhibitory function of M1 (Kujirai *et al.* 1993), remained unchanged; SICF and ICF were enhanced by QPS-5 ms whereas reduced by QPS-50 ms (Hamada *et al.* 2008*a*). Based on the hypothesis of the mechanism of SICF (Hanajima *et al.* 2002), it is possible that QPS changes the quantity of EPSPs in excitatory circuits responsible for SICF (Hamada *et al.* 2008*a*). These results led us to surmise that the mechanism of QPS-induced plasticity involves synaptic plasticity in the excitatory circuits of M1 with features of non-linear dependence on the ISI of QPS, suggesting the presence of threshold for LTP- and LTD-like plasticity induction in line with previous findings of synaptic plasticity (Dudek & Bear, 1992).

Possible mechanisms of effects of priming over SMA on QPS-induced plasticity

The present results suggest that SMA priming influenced subsequent induction of synaptic plasticity in the excitatory circuits of M1. Priming over SMA elicited bidirectional shifts of the crossover point of the stimulus–response function of motor cortical plasticity (Fig. 5). The priming effects depended on the precise parameters of priming stimulation which specifically and transiently altered SICF without significant changes in MEP. We note that at least three possible mechanisms might account for the present findings: metaplasticity (Abraham & Bear, 1996), a gating mechanism (Ziemann & Siebner, 2008) and state-dependent effects (Fujiwara & Rothwell, 2004; Huang *et al.* 2008).

SMA priming-induced metaplasticity

First, it might be possible to interpret these findings within the framework of metaplasticity, or the plasticity of synaptic plasticity, in which neural activity at one point in time can change cells or synapses such that their ability to exhibit LTP or LTD after a later bout of activity is altered (Abraham, 2008). Metaplasticity is best documented by showing that an experimental manipulation which itself causes no persistent synaptic plasticity can nevertheless produce a shift in the crossover point of the frequency–response function of synaptic plasticity induced by a period of conditioning stimulation (Abraham, 2008). More specifically, if a manipulation reduces LTP then this should reflect elevation of the induction threshold for LTP; thus, the frequency of the conditioning stimulation required to produce LTP becomes higher, compatible with a shift in the crossover point of LTP and LTD in the conditioning frequency–response curve (Wang & Wagner, 1999; Zhang *et al.* 2005).

In this context, QPS-5 ms priming over SMA transiently enhances SICF, and this prior history of cortical activity elevated the threshold for inducing LTP-like plasticity. This is confirmed by the observation that QPS-5 ms priming over SMA did not occlude LTP-like plasticity by QPS-1.5 ms, whereas the same priming interfered with LTP-like plasticity induced by QPS-5 ms and QPS-10 ms, which produced LTD-like plasticity instead. These results indicate elevation of the threshold of LTP-like plasticity induction. In fact, QPS-5 ms priming over SMA shifted the crossover point of the stimulus–response function to the right along the x-axis (Fig. 5).

Theoretically, enhancement of prior neuronal activity should promote LTD (Bienenstock *et al.* 1982). This is confirmed by the fact that QPS-30 ms with QPS-5 ms priming produced a lasting decrease of MEP sizes as compared to QPS-30 ms without priming (Fig. 3*D*). However, LTD-like plasticity induced by QPS-50 ms and QPS-100 ms were not enhanced although the duration of suppression was shortened by QPS-5 ms priming over SMA. The disparity may be partly explained by previous studies of metaplasticity which revealed that the balance of NMDA receptor subunits (i.e. NR2A and NR2B) is one important factor in modulating the threshold for synaptic plasticity (Philpot *et al.* 2003, 2007). Some forms of metaplasticity are NMDA receptor dependent (Huang *et al.* 1992; Christie & Abraham, 1992; Abraham & Huggett, 1997; Zhang *et al.* 2005), and the ratio of NR2A/2B, which is increased by prior cortical activity, elevates the thresholds for both LTP and LTD induction (Yashiro & Philpot, 2008). Perhaps a similar mechanism is implicated in our present observation that QPS-5 ms priming over SMA elevates the thresholds for both LTP- and LTD-like plasticity.

In contrast, after QPS-50 ms priming over SMA, which transiently reduced SICF, LTP-like plasticity was induced by QPS-30 ms, which had produced transient MEP suppression when given alone. Indeed our results are compatible with the view that metaplastic changes can best be recognized by using a near-threshold stimulation regimen (i.e. near the crossover point) (Christie *et al.* 1995) since QPS-50 ms priming over SMA did not interfere with LTP- or LTD-like plasticity induced by QPS-10 ms or QPS-100 ms (Fig. 5). One result is apparently at odds with this explanation though; QPS-50 ms priming over SMA erased LTP-like plasticity usually seen after the QPS-5 ms protocol. According to the BCM rule, LTP-like plasticity should be enhanced after QPS-50 ms priming since it transiently reduced cortical activity. One possible explanation comes from animal studies of metaplasticity which suggest an inverted U-shaped relation between the amount of TBS and the degree of LTP (Christie *et al.* 1995; Abraham & Huggett, 1997). Such time-dependent LTP reversal process or overstimulation effect has been believed to be a normal feature of LTP induction, probably caused by a depotentiation mechanism during the massed presentation of tetanic stimulation (Christie *et al.* 1995; Abraham & Huggett, 1997). These authors found that only two trains of TBS were required to induce LTP but eight trains of TBS, which induce LTP on its own, were unable to induce LTP with low-frequency priming stimulation. This blocking of LTP has been suggested to reflect the overstimulation effect (Christie *et al.* 1995). We suggest that similarly, the present results might reflect comparable overstimulation effects with priming stimulation.

One conspicuous point of our results is that the SICF was modulated transiently by the priming stimulation alone. Thus, the effects of SMA priming on SICF could have returned to baseline by the time QPS was delivered following the collection of 20 MEPs at B1. This is consistent with our previous study showing transient modulation of SICF with priming over M1 (Hamada *et al.* 2008*a*). We favour the view that this transient modulation of SICF reflects prior history of cortical activity and that such prior activity substantially influences subsequent QPS-induced plasticity in a metaplastic manner (Hamada *et al.* 2008*a*). However, it is still possible that such transient modulation of SICF has a weak association with the priming effects because the time course of the influence on SICF did not parallel that of the priming effect.

Previous human studies demonstrated the effects of priming stimulation on subsequent rTMS-induced plasticity, indicating metaplasticity (Iyer *et al.* 2003; Lang *et al.* 2004; Siebner *et al.* 2004; Müller *et al.* 2007; Ragert *et al.* 2009). We have also shown metaplastic changes of QPS-induced plasticity by priming stimulation (Hamada *et al.* 2008*a*). In the previous reports, both priming and conditioning were applied over M1 using exactly the same stimulus intensity, suggesting that they modulated the same synaptic connections (Hamada *et al.* 2008*a*). According to animal experiments showing homosynaptic and heterosynaptic metaplasticity (Wang & Wagner, 1999; Abraham *et al.* 2001), our previous results indicate that the homeostatic changes were mediated via homosynaptic mechanism of metaplasticity. In contrast to the previous studies, in the present work priming was applied over SMA, leading to bidirectional modulation of SICF, whereas the subsequent conditioning was applied over M1. It is reasonable to believe that the synapses in M1 that are altered by the SMA priming are those involved in a SMA–M1 projection, and that these are likely to be partially different from those modulated by conditioning over M1. This raises the intriguing possibility that the effects of priming can be ascribed to a mixture of homosynaptic and heterosynaptic metaplasticity. Another implication from this paper is that SMA priming would have metaplastic effects on subsequent rTMS-induced plasticity of M1 which can be produced by any rTMS protocols that are capable of inducing LTP- and LTD-like changes.

Gating mechanism and state-dependent effect

Although we favour a metaplasticity theory to account for the present findings, other mechanisms might be involved. One possibility is a gating mechanism (Ziemann & Siebner, 2008); if QPS-5 ms priming had increased intracortical inhibition, then it might have rendered subsequent QPS conditioning less effective in exciting cortical output neurons trans-synaptically. In such a case, each burst of QPS would have produced a smaller amount of calcium

influx into the neurons, resulting in induction of LTD-like plasticity. However, neither SICI nor LICI was altered by priming over SMA, thus leading to the tentative conclusion that it is much less likely that the priming effects arise as a consequence of the alteration of intracortical inhibitory circuits.

Another possible explanation is related to several human studies in which voluntary contraction influences rTMS-induced plasticity (Fujiwara & Rothwell, 2004; Gentner *et al.* 2008; Huang *et al.* 2008). The after-effects of rTMS depend on the state of the cortex at the time the stimulation is applied. Thus, the effect of 5 Hz rTMS on SICI was reversed by muscle contraction during rTMS (Fujiwara & Rothwell, 2004). More recently, voluntary contraction during TBS abolished TBS-induced plasticity (Huang *et al.* 2008). Huang *et al.* (2008) proposed two possibilities to account for such state-dependent effects. First, the voluntary contraction perhaps changes the membrane potential or Ca^{2+} concentration of pyramidal neurons, directly affecting TBS-induced plasticity. 'Busy line' effects are another possible explanation; given that synapses stimulated by TBS are the same as those activated by voluntary contraction, extra activation of those synapses by TBS is negligible (Huang *et al.* 2008). Yet another study showed that voluntary contraction of sufficient duration changes the direction of TBS-induced plasticity; the authors contrastingly interpret their findings within the framework of metaplasticity theory (Gentner *et al.* 2008). Perhaps it is still an open question regarding the mechanism of effects of voluntary contraction on TBS-induced plasticity. In any case, SMA priming which produced changes in SICF might be a sign of some sort of baseline difference in the state of motor cortex independent of metaplasticity, resulting in alteration of subsequent QPS-induced plasticity.

SMA–M1 interplay and metaplasticity

Experimental observations of metaplasticity are considered to represent a major form of homeostatic mechanism of synaptic plasticity that prevents neuronal circuits from becoming destabilized and that maintains them within a dynamic range of modifiability (Abbott & Nelson, 2000; Abraham, 2008). Our findings might therefore highlight a homeostatic (or metaplastic) regulation of synaptic plasticity within excitatory circuits of M1 by input from SMA. Since SMA is implicated in higher motor control and the learning process (Luppino *et al.* 1993; Tanji & Shima, 1994; Tanji, 1996; Hikosaka *et al.* 1999; Nachev *et al.* 2008), the present results further raise the intriguing possibility that a preceding period of learning which entails a change in neuronal activity of SMA may regulate subsequent learning that is handled by neuronal circuits of M1 (Hikosaka *et al.* 1999; Sane & Donoghue, 2000). Since this study was not designed to test this hypothesis, future studies would be needed to shed light on possible metaplastic interplay between SMA and M1 during motor learning.

Finally, the shortcoming of the present study is that the lack of direct recording of synaptic responses in conscious humans renders any hypothesis about the precise neuronal mechanisms underlying QPS-induced plasticity or metaplasticity speculative (Cooke & Bliss, 2006). However, although the interpretation of the present data is inferential, the present study does suggest strongly that there may be important interactions between M1 and SMA in terms of metaplasticity.

Conclusions

Preceding stimulation over SMA elicited bidirectional shifts of the crossover point of the stimulus–response function of subsequent motor cortical plasticity. SMA priming transiently altered the synaptic efficiencies of excitatory circuits within M1. The data support the view that the homeostatic changes are mediated via mechanisms of metaplasticity. These findings highlight an important interplay between M1 and SMA regarding metaplasticity which might underpin learning and memory processes.

References

Abbott LF & Nelson SB (2000). Synaptic plasticity: taming the beast. *Nat Neurosci* **3**, 1178–1183.

Abraham WC (2008). Metaplasticity: tuning synapses and networks for plasticity. *Nat Rev Neurosci* **9**, 387–399.

Abraham WC & Bear MF (1996). Metaplasticity: the plasticity of synaptic plasticity. *Trends Neurosci* **19**, 126–130.

Abraham WC & Huggett A (1997). Induction and reversal of long-term potentiation by repeated high-frequency stimulation in rat hippocampal slices. *Hippocampus* **7**, 137–145.

Abraham WC, Mason-Parker SE, Bear MF, Webb S & Tate WP (2001). Heterosynaptic metaplasticity in the hippocampus *in vivo*: a BCM-like modifiable threshold for LTP. *Proc Natl Acad Sci U S A* **98**, 10924–10929.

Abraham WC & Tate WP (1997). Metaplasticity: a new vista across the field of synaptic plasticity. *Prog Neurobiol* **52**, 303–323.

Akkal D, Dum RP & Strick PL (2007). Supplementary motor area and presupplementary motor area: targets of basal ganglia and cerebellar output. *J Neurosci* **27**, 10659–10673.

Bienenstock EL, Cooper LN & Munro PW (1982). Theory for the development of neuron selectivity: Orientation specificity and binocular interaction in visual cortex. *J Neurosci* **2**, 32–48.

Chen R, Samii A, Canos M, Wassermann EM & Hallett M (1997). Effects of phenytoin on cortical excitability in humans. *Neurology* **49**, 881–883.

Christie BR & Abraham WC (1992). Priming of associative long-term depression by θ frequency synaptic activity. *Neuron* **9**, 79–84.

Christie BR, Stellwagen D & Abraham WC (1995). Reduction of the threshold for long-term potentiation by prior theta-frequency synaptic activity. *Hippocampus* **5**, 52–59.

Civardi C, Cantello R, Asselman P & Rothwell JC (2001). Transcranial magnetic stimulation can be used to test connections to primary motor areas from frontal and medial cortex in humans. *Neuroimage* **14**, 1444–1453.

Cooke SF & Bliss VP (2006). Plasticity in the human central nervous system. *Brain* **129**, 1659–1673.

Dudek SM & Bear MF (1992). Homosynaptic long-term depression in area CA1 of hippocampus and the effects of N-methyl-D-aspartate receptor blockade. *Proc Natl Acad Sci U S A* **89**, 4363–4367.

Dum RP & Strick PL (1991). The origin of corticospinal projections from the premotor areas in the frontal lobe. *J Neurosci* **11**, 667–689.

Dum RP & Strick PL (1996). Spinal cord terminations of the medial wall motor areas in macaque monkeys. *J Neurosci* **16**, 6531–6525.

Drummond GB (2009). Reporting ethical matters in *The Journal of Physiology*: standards and advice. *J Physiol* **587**, 713–719.

Fujiwara T & Rothwell JC (2004). The after effects of motor cortex rTMS depend on the state of contraction when rTMS is applied. *Clin Neurophysiol* **115**, 1514–1518.

Gentner R, Wankerl K, Reinsberger C, Zeller D & Classen J (2008). Depression of human corticospinal excitability induced by magnetic theta-burst stimulation: evidence of rapid polarity-reversing metaplasticity. *Cereb Cortex* **18**, 2046–2053.

Hallett M (2007). Transcranial magnetic stimulation: A primer. *Neuron* **55**, 187–199.

Hamada M, Hanajima R, Terao Y, Arai N, Furubayashi T, Inomata-Terada S *et al.* (2007). Quadro-pulse stimulation is more effective than paired-pulse stimulation for plasticity induction of the human motor cortex. *Clin Neurophysiol* **118**, 2672–2682.

Hamada M, Terao Y, Hanajima R, Shirota Y, Nakatani-Enomoto S, Furubayashi T, Matsumoto H & Ugawa Y (2008*a*). Bidirectional long-term motor cortical plasticity and metaplasticity induced by quadripulse transcranial magnetic stimulation. *J Physiol* **586**, 3927–3947.

Hamada M, Ugawa Y, Tsuji S & Effectiveness of rTMS on Parkinson's Disease Study Group, Japan (2008*b*). High-frequency rTMS over the supplementary motor area for treatment of Parkinson's disease. *Mov Disord* **23**, 1524–1531.

Hanajima R, Ugawa Y, Terao Y, Enomoto H, Shiio Y, Mochizuki H *et al.* (2002). Mechanisms of intracortical I-wave facilitation elicited with paired-pulse magnetic stimulation in humans. *J Physiol* **538**, 253–261.

Hikosaka O, Nakahara H, Rand MK, Sakai K, Lu X, Nakamura K, Miyachi S & Doya K (1999). Parallel neural networks for learning sequential procedures. *Trends Neurosci* **22**, 464–471.

Hikosaka O, Sakai K, Miyauchi S, Takino R, Sasaki Y & Putz B (1996). Activation of human presupplementary motor area in learning of sequential procedures: a functional MRI study. *J Neurophysiol* **76**, 617–621.

Huang YY, Colino A, Selig DK & Malenka RC (1992). The influence of prior synaptic activity on the induction of long-term potentiation. *Science* **255**, 730–733.

Huang YZ, Chen RS, Rothwell JC & Wen HY (2007). The after-effect of human theta burst stimulation is NMDA receptor dependent. *Clin Neurophysiol* **118**, 1028–1032.

Huang YZ, Rothwell JC, Edwards MJ & Chen RS (2008). Effect of physiological activity on NMDA-dependent form of cortical plasticity in human. *Cereb Cortex* **18**, 563–570.

Inase M, Tokuno H, Nambu A, Akazawa T & Takada M (1999). Corticostriatal and corticosubthalamic input zones from the presupplementary motor area in the macaque monkey: comparison with the input zones from the supplementary motor area. *Brain Res* **833**, 191–201.

Iyer MB, Schleper N & Wassermann EM (2003). Priming stimulation enhances the depressant effect of low frequency repetitive transcranial magnetic stimulation. *J Neurosci* **23**, 10867–10872.

Kaneda K, Nambu A, Tokuno H & Takada M (2002). Differential processing patterns of motor information via striatopallidal and striatonigral projections. *J Neurophysiol* **88**, 1420–1432

Kujirai T, Caramia MD, Rothwell JC, Day BL, Thompson PD, Ferbert A, Woe O, Asselman P & Marsden CD (1993). Corticocortical inhibition in human motor cortex. *J Physiol* **471**, 501–519.

Lang N, Siebner HR, Ernst D, Nitsche MA, Paulus W, Lemon RN & Rothwell JC (2004). Preconditioning with transcranial direct current stimulation sensitizes the motor cortex to rapid-rate transcranial magnetic stimulation and controls the direction of after-effects. *Biol Psychiatry* **56**, 634–639.

Lee KM, Chang KH & Roh JK (1999). Subregions within the supplementary motor area activated at different stages of movement preparation and execution. *Neuroimage* **9**, 117–123.

Luppino G, Matelli M, Camarda R & Rizzolatti G (1993). Corticocortical connections of area F3 (SMA-proper) and area F6 (pre-SMA) in the macaque monkey. *J Comp Neurol* **338**, 114–140.

McAllister SMA, Rothwell JC & Ridding MC (2009). Selective modulation of intracortical inhibition by low-intensity theta burst stimulation. *Clin Neurophysiol* **120**, 820–826.

Matsunaga K, Maruyama A, Fujiwara T, Nakanishi R, Tsuji S & Rothwell JC (2005). Increased corticospinal excitability after 5 Hz rTMS over the supplementary motor area. *J Physiol* **562**, 295–306.

Mavroudakis N, Caroyer JM, Brunko E & Zegers de Beyl D (1994). Effects of diphenylhydantoin on motor potentials evoked with magnetic stimulation. *Electroencephalogr Clin Neurophysiol* **93**, 428–433.

Mavroudakis N, Caroyer JM, Brunko E & Zegers de Beyl D (1997). Effects of vigabatrin on motor potentials with magnetic stimulation. *Electroencephalogr Clin Neurophysiol* **105**, 124–127.

Müller JF, Orekhov Y, Liu Y & Ziemann U (2007). Homeostatic plasticity in human motor cortex demonstrated by two consecutive sessions of paired associative stimulation. *Eur J Neurosci* **25**, 3461–3468.

Nachev P, Kennard C & Husain M (2008). Functional role of the supplementary and pre-supplementary motor areas. *Nat Rev Neurosci* **9**, 856–869.

Okabe S, Ugawa Y, Kanazawa I & Effectiveness of rTMS on Parkinson's Disease Study Group (2003). 0.2-Hz repetitive transcranial magnetic stimulation has no add-on effects as compared to a realistic sham stimulation in Parkinson's disease. *Mov Disord* **18**, 382–388.

Oldfield RC (1971). The assessment and analysis of handedness: the Edinburgh inventory. *Neuropsychologia* **9**, 97–113.

Philpot BD, Cho KK & Bear MF (2007). Obligatory role of NR2A for metaplasticity in visual cortex. *Neuron* **53**, 495–502.

Philpot BD, Espinosa JS & Bear MF (2003). Evidence for altered NMDA receptor function as a basis of metaplasticity in visual cortex. *J Neurosci* **23**, 5583–5588.

Ragert P, Camus M, Dimyan MA, Vandermeeren Y & Cohen LG (2009). Modulation of iTBS effects applied over primary motor cortex (M1) by conditioning stimulation of the opposite M1. *J Neurophysiol* **102**, 766–773.

Reis J, Swayne OB, Vandermeeren Y, Camus M, Dimyan MA, Harris-Love M *et al.* (2008). Contribution of transcranial magnetic stimulation to the understanding of cortical mechanisms involved in motor control. *J Physiol* **586**, 325–351.

Rizzo V, Siebner HR, Modugno N, Pesenti A, Munchau A, Gerschlager W, Webb RM & Rothwell JC (2004). Shaping the excitability of the human motor cortex with premotor rTMS. *J Physiol* **554**, 483–495.

Rossini PM, Barker AT, Berardelli A, Caramia MD, Caruso G, Cracco RQ *et al.* (1994). Non-invasive electrical and magnetic stimulation of the brain, spinal cord and roots: basic principles and procedures for routine clinical application. Report of an IFCN committee. *Electroencephalogr Clin Neurophysiol* **91**, 79–92.

Sane JN & Donoghue (2000). Plasticity and primary motor cortex. *Ann Rev Neurosci* **23**, 393–415.

Serrien DJ, Strens LH, Oliviero A & Brown P (2002). Repetitive transcranial magnetic stimulation of the supplementary motor area (SMA) degrades bimanual movement control in humans. *Neurosci Lett* **328**, 89–92.

Siebner HR, Lang N, Rizzo V, Nitsche MA, Paulus W, Lemon RN & Rothwell JC (2004). Preconditioning of low-frequency repetitive transcranial magnetic stimulation with transcranial direct current stimulation: Evidence for homeostatic plasticity in the human motor cortex. *J Neurosci* **24**, 3379–3385.

Stefan K, Kunesch E, Benecke R, Cohen LG & Classen J (2002). Mechanisms of enhancement of human motor cortex excitability induced by interventional paired associative stimulation. *J Physiol* **543**, 699–708.

Tanji J (1996). New concepts of the supplementary motor area. *Curr Opin Neurobiol* **6**, 782–787.

Tanji J & Shima K (1994). Role for supplementary motor area cells in planning several movements ahead. *Nature* **371**, 413–416.

Terao Y, Ugawa Y, Enomoto H, Furubayashi T, Shiio Y, Machii K *et al.* (2001). Hemispheric lateralization in the cortical motor preparation for human vocalization. *J Neurosci* **21**, 1600–1609.

Tokimura H, Ridding MC, Tokimura Y, Amassian VE & Rothwell JC (1996). Short latency facilitation between pairs of threshold magnetic stimuli applied to human motor cortex. *Electroencephalogr Clin Neurophysiol* **101**, 263–272.

Tokuno H & Nambu A (2000). Organization of nonprimary motor cortical inputs on pyramidal and nonpyramidal tract neurons of primary motor cortex: An electrophysiological study in the macaque monkey. *Cereb Cortex* **10**, 58–68.

Valls-Sole J, Pascual-Leone A, Wassermann EM & Hallett M (1992). Human motor evoked responses to paired transcranial magnetic stimuli. *Electroencephalogr Clin Neurophysiol* **85**, 355–364.

Verwey W, Lammens R & van Honk J (2002). On the role of the SMA in the discrete sequence production task: a TMS study. *Neuropsychologia* **40**, 1268–1276.

Wang H & Wagner JJ (1999). Priming-induced shift in synaptic plasticity in the rat hippocampus. *J Neurophysiol* **82**, 2024–2028.

Wassermann EM (1998). Risk and safety of repetitive transcranial magnetic stimulation: report and suggested guidelines from the International Workshop on the Safety of Repetitive Transcranial Magnetic Stimulation, June 5–7, 1996. *Electroencephalogr Clin Neurophysiol* **108**, 1–16.

Wassermann EM, Samii A, Mercuri B, Ikoma K, Oddo D, Grill SE & Hallett M (1996). Responses to paired transcranial magnetic stimuli in resting, active, and recently activated muscles. *Exp Brain Res* **109**, 158–163.

Yashiro K & Philpot BD (2008). Regulation of NMDA receptor subunit expression and its implications for LTD, LTP, and metaplasticity. *Neuropharmacol* **55**, 1081–1094.

Zhang L, Kirschstein T, Sommerberg B, Merkens M, Manahan-Vaughan D, Elpersma Y & Beck H (2005). Hippocampal synaptic metaplasticity requires inhibitory autophosphorylation of Ca^{2+}/calmodulin-dependent kinase II. *J Neurosci* **25**, 7697–7707.

Ziemann U, Iliac TV, Pauli C, Meintzschel F & Ruge D (2004). Learning modifies subsequent induction of long-term potentiation-like and long-term depression-like plasticity in human motor cortex. *J Neurosci* **24**, 1666–1672.

Ziemann U, Lönnecker S, Steinhoff BJ & Paulus W (1996). Effects of antiepileptic drugs on motor cortex excitability in humans: a transcranial magnetic stimulation study. *Ann Neurol* **40**, 367–378.

Ziemann U & Siebner HR (2008). Modifying motor learning through gating and homeostatic metaplasticity. *Brain Stim* **1**, 60–66.

Ziemann U, Tergau F, Wassermann EM, Wischer S, Hildebrandt J & Paulus W (1998). Demonstration of facilitatory I-wave interaction in the human motor cortex by paired transcranial magnetic stimulation. *J Physiol* **511**, 181–190.

Author contributions

M.H. and Y.U. contributed to the conception and design of the experiments. M.H. performed the experiments and analysed the data. All authors participated in data interpretation. M.H., Y.T. and Y.U. wrote the manuscript. All authors revised the manuscript and approved the final manuscript. The experiments were performed at Department of Neurology, the University of Tokyo, Japan.

Acknowledgements

M.H. is a research fellow of the Japan Society for the Promotion of Science, Tokyo, Japan. We are grateful to Professor John Rothwell for his constructive comments and English editing. We also thank Mr Mikio Asano and Mr Tsukasa Kajiwara for technical assistance. Part of this work was supported by Research Project Grants-in-aid for Scientific Research No. 18590928 (Y.T.) and No. 17590865 (R.H.) from the Ministry of Education, Culture, Sports, Science and Technology of Japan, the Research Committee on rTMS Treatment of Movement Disorders from the Ministry of Health, Labour and Welfare of Japan (17231401), the Research Committee on Dystonia, the Ministry of Health, Labour and Welfare of Japan, the Committee of the Study of Human Exposure to Electromagnetic Fields, Ministry of Internal Affairs and Communications, the Life Science Foundation of Japan, and the Magnetic Health Science Foundation.

ジストニアに対する各治療法の位置づけ1
——自験例に基づく保存的治療法の検討——

佐光 亘[1]／島津 秀紀[1]／村瀬 永子[1]／松崎 和仁[2]／西田 善彦[3]
永廣 信治[2]／梶 龍兒[1]／後藤 惠[1]

Treatment of dystonia 1 —the investigation of conservative therapy based on our experience—

Wataru Sako[1] / Hideki Shimazu[1] / Nagako Murase[1] / Kazuhito Matsuzaki[2] / Yoshihiko Nishida[3]
Shinji Nagahiro[2] / Ryuji Kaji[1] / Satoshi Goto[1]

Abstract: Dystonia is characterized by sustained muscle contractions that produce repetitive twisting movements and abnormal postures, caused by abnormality of extrapyramidal tract. We have some options to treat these symptoms, however, clear protocol for selection of treatment remain to be established. Based on our experience, we reported here the strategy of the conservative therapy for dystonia including oral administration, botulinum toxin (BTX), muscle afferent block (MAB) and repetitive transcranial magnetic stimulation (rTMS).

Keywords: dystonia, botulinum toxin (BTX), muscle afferent block (MAB)

1 徳島大学大学院 ヘルスバイオサイエンス研究部 神経情報医学分野〔Department of Clinical Neuroscience, Institute of Health Biosciences, Graduate School of Medicine, University of Tokushima〕
〒770-8503 徳島市蔵本町 3-18-15 / TEL: 088-633-7207 / FAX: 088-633-7208
2 徳島大学大学院 ヘルスバイオサイエンス研究部 脳神経外科学分野〔Department of Neurosurgery, Institute of Health Biosciences, Graduate School of Medicine, University of Tokushima〕
〒770-8503 徳島市蔵本町 3-18-15 / TEL: 088-631-3111 / FAX: 088-632-9464
3 いちえ会伊月病院 神経内科〔Itsuki hospital, Neurology〕〒770-0852 徳島市徳島町 2-54 / TEL: 088-622-1117

機能的脳神経外科 48 (2009) 40–41

背　景

ジストニアは錐体外路系の異常に基づき筋緊張の異常をきたす疾患である。いくつかの治療法が存在するが，その選択に関して明確な基準はない。今回我々は，保存的治療法に焦点を絞り，関連施設で経験した有効例をいくつか抽出し，各治療法のジストニア治療における意義について検討した。

各治療法と症例

徳島大学病院および関連2施設（医仁会武田総合病院，伊月病院）で筆者らが行っているジストニア外来の2007年度延べ受診者数は3,329名であった。原発性ジストニア自験例における相対頻度は罹患部位による分類を用いると，局所性ジストニア91.1%，分節性ジストニア7.2%，多巣性ジストニア0.6%，全身性ジストニア1.2%であり，その9割を局所性ジストニアが占める。局所性ジストニアの内訳は，眼瞼痙攣32.6%，痙性斜頸38.2%，書痙・上肢ジストニア16.5%，その他3.8%であった。これらのサブタイプに応じて内服治療，ボツリヌス毒素治療（BTX），Muscle Affferent Block（MAB）治療，経頭蓋磁気刺激治療（rTMS），脳深部刺激術（DBS）のいずれかが選択されるが，今回は保存的治療法である前4者に焦点を絞り，有効症例を抽出し，各治療法の位置づけについて検討した。

(1) 内服治療

すべてのタイプのジストニアに対して内服治療が試みられる。トリヘキシフェニジルを第一選択とし，適宜クロナゼパム・ジアゼパムなどが第二選択薬として追加される。いずれの薬剤も効果不十分であることが多いが，時に内服治療のみで満足いく結果が得られることもある。

症例1：guitarist's cramp，50歳，男性。ギターを弾く時に，右第4/5指の伸展が見られたが，トリヘキシフェニジル6 mg/day投与で症状改善。

(2) BTX

痙性斜頸，眼瞼痙攣に対しては，症状の改善が明らかに優れているBTX治療を第一選択とする。特に前者において，若年発症・早期導入例では寛解誘導の可能性もあり，積極的に導入する。

症例2：痙性斜頸，24歳，男性。頸部左回旋後屈を呈し，発症3ヵ月で受診し，BTX，トリヘキシフェニジルによる治療開始し，約1年後に完全寛解し，治療終了となった。

(3) MAB

BTXに適応のない四肢・体幹（傍脊柱筋は除く）の筋群に生じたジストニアに対して適応がある。MABは0.5%リドカインにその1/10量以下のエタノールを加えたものを罹患筋に注入する治療法である。0.5%リドカインの総量は50 ml以

Table 1 Strategy of the conservative therapy for dystonia

1．局所性ジストニア
・瘤性斜頸・眼瞼痙攣：BTX・内服併用
・上肢ジストニア：内服→MAB　BTX and/or rTMS
・下肢・体幹ジストニア：MAB・内服併用→BTX
2．多巣性・分節性・全身性ジストニア
・罹患部位ごとに上記治療法の併用

下，1筋あたり25 ml以下にして使用することが多いが，リドカインのみでもある程度の効果が期待できる。明らかな改善が得られる場合にBTXを追加する場合もある。

症例3：hand dystonia，35歳，女性。キーボード入力の職に就いていたが，入力時に右手首の屈曲，手指こわばりを自覚し，発症3年目で受診となった。トリヘキシフェニジル内服とともに，MAB治療を開始した。上記治療法有効であり，さらにBTXも追加し，上記症状は改善した。

症例4：軸性ジストニア，55歳，女性。養豚農家を経営していたが，頸部～体幹の右前側屈を発症し，トリヘキシフェニジル，クロナゼパム内服治療とともにMAB治療を開始した。上記治療が有効であり，さらにBTXも併用し，治療開始より約1年で上記症状はほぼ消失した。

(4) rTMS

内服・MABに抵抗性の書痙・職業性痙攣など上肢ジストニアに対しては，可能であればrTMSの検討を行う。有効率は決して高いとは言えないが，思わぬ改善と長期効果が得られる場合があり完全寛解例も存在するため，DBSを選択する前に試みられてもよい。

まとめ

ジストニアは病因と罹患部位により分類される。いずれのタイプにも適応のある内服治療を除く保存的治療の選択に関しては，病因ではなく罹患部位によって決定される。瘤性斜頸や眼瞼痙攣ではBTXの有効性は明白であり，BTXが第一選択になりうる。上肢のジストニアに関しては，まずはMABを行い，有効例に対してBTXを併用する。DBSの適応を検討する前に，rTMSを試みてもよい。下肢・体幹のジストニアでもMABをまず行い，改善が認められた症例に対してBTXを使用する。また，多巣性・分節性・全身性ジストニアでは罹患部位ごとに上記治療法の併用を行う。上記治療戦略をTable 1にまとめた。

文献

1) Jankovic J: Treatment of dystonia. Lancet Neurol 5: 864-872, 2006.
2) Zesiewicz TA et al: Botulinum toxin A for the treatment of cervical dystonia. Exp Opin Pharmacol 5: 2017-2024, 2004.
3) Kaji R et al: Tonic vibration reflex and muscle afferent block in writer's cramp. Ann Neurol 38: 155-162, 1995.
4) Murase N et al: Subthreshold low-frequency repetitive transcranial magnetic stimulation over the premotor cortex modulates writer's cramp. Brain 128: 104-115, 2005.

BRAIN and NERVE 61(1) : 65-71, 2009

原　著
Original Article

痙性斜頸患者における Toronto Western Spasmodic Torticollis Rating Scale (TWSTRS) の評価者間信頼性の検討

梶　龍兒[1)]　大澤美貴雄[2)]　柳澤信夫[3)]
TWSTRS 評価者間信頼性検討会[4)]

Inter-rater Reliability while Using the Toronto Western Spasmodic Torticollis Rating Scale (TWSTRS) in Patients with Cervical Dystonia

Ryuji Kaji[1)], Mikio Osawa[2)], Nobuo Yanagisawa[3)]

Abstract

We examined the inter-rater reliability for the evaluation of patients with cervical dystonia by using the Toronto Western Spasmodic Torticollis Rating Scale (TWSTRS) (translated into Japanese). The TWSTRS is a rating scale that assesses patients with cervical dystonia by grading their symptoms on a subscale of severity, disability, and pain. This study used to TWSTRS-severity scores to examine the inter-rater reliability among 27 evaluators (neurologists) by using videotaped images of 2 patients.

Along with the total-severity score on the TWSTRS, the intra-class correlation (ICC) and the lower limit of the 95% confidence interval were calculated as indices of inter-rater reliability. A high ICC of 0.745 was obtained. The ICC obtained from another study conducted outside Japan was 0.763, which is almost equivalent to the result of our study. Thus, the TWSTRS has a favorable inter-rater reliability which suggests that this scale was sufficiently reliable to be used as an accurate and easily available rating tool during the treatment of cervical dystonia.

(Received: December 19, 2006, Accepted: September 29, 2008)

Key words : TWSTRS, cervical dystonia, ICC, inter-rater reliability

はじめに；研究目的と背景

痙性斜頸は，頸部筋の不随意的な収縮により引き起こされる頭頸部の不随意運動あるいは異常姿勢のことをいう。有病率は，日本では10万人あたり2.85人[1)]，米国では10万人あたり9人[2)]あるいは30人[3)]との報告があり，日本よりも頻度は高い。診断基準は「頭頸部の筋緊張異常により頭位の異常を生じる病態」と定義され，日本においては欧米の定義が翻訳されて使用されている。また，治療の第一選択は世界的にボツリヌス毒素療法[4-6)]とされていることからも，日本と欧米で医療環境に大きな違いはないと考えられる。

痙性斜頸に対する有効な治療薬を開発するために客観

1) 徳島大学大学院ヘルスバイオサイエンス研究部神経情報医学分野〔〒770-8503　徳島県徳島市蔵本町3-18-15〕Department of Clinical Neuroscience, Institute of Health Biosciences, The University of Tokushima Graduate School, 3-18-15 Kuramoto-cho, Tokushima 770-8503, Japan
2) 東京女子医科大学病院神経内科　Department of Neurology, Tokyo Women's Medical University
3) 関東労災病院　Kanto Rosai Hospital
4) 参加施設および医師名を本文末に掲載

1881-6096/09/¥500/論文/JCLS

Table 1 Items of TWSTRS -severity Scale

A 1．回旋（右旋および左旋）	B．偏倚持続
A 2．側屈	C．感覚トリック
A 3．a）前屈またはb）後屈	D．肩挙上または肩の前方偏倚
A 4．側方偏倚	E．自動運動域
A 5．前後偏倚	F．頭位を正常に維持できる時間

的な評価尺度を用いることが重要になっている。痙性斜頸治療の評価尺度として，海外ではToronto Western Spasmodic Torticollis Rating Scale (TWSTRS)[7]が治療効果の評価に用いられている。一般に，海外で作成された評価尺度を本邦で使用する場合，日本語への正確な翻訳が必須となるが，原著の意味を忠実に再現する訳語を当てはめることはしばしば困難である。したがって，使用する評価尺度によっては，例えば地域特有の質問などが含まれる場合には，事前にその日本語版の信頼性や妥当性を評価しておくことが重要である。

TWSTRS[7]は1994年にConskiとLangによって開発された評価尺度であり，重症度，機能障害度および疼痛度を評価する3つの下位尺度から構成されている。このうち重症度スケールにおける信頼性および妥当性が報告されている。重症度スケールは本尺度の主要な構成要素であり，頭位偏倚の角度や偏倚の持続時間を評価するために用いられる。すなわち海外や日本とで共通した概念である「角度」や「時間」を評価の基準としているため，測定者間における評価の不一致などは少ないと考えられる。しかしながら，本邦では本尺度の使用経験がないためこれを裏付ける十分なデータは得られていない。そこで，米国において詳細な評価者訓練マニュアルが提示されているTWSTRS-重症度スケールについて，本邦における評価者間一致性を検討した。

I．研究方法

1．評価対象とした映像

トレーニングに使用するビデオテープは，TWSTRSの開発者が企画し，4名の運動障害の専門家が，Athena Neurosciences（現エラン社）から教育助成金を受けて共同で制作したものである。収録されたトレーニング用の患者映像例は，上記専門家のうち3名が，20例の痙性斜頸患者のビデオ映像例について独立に評価し，少なくとも3名中2名の評価者のスコアが一致し，残り1名のスコアが他の2名のスコアから1ポイントしかずれていなかった患者例を用いている。

評価者間信頼性検討に使用する2名の患者映像例は，上述の映像例とともに，評価者トレーニング用に作成されたTWSTRSビデオテーププロトコルを用いて収録されたものである。

なお，本ビデオテープの日本語版は，科学技術翻訳専門の訳者によって原著から翻訳され，痙性斜頸の治療に精通した神経内科医によって訳語がチェックされた。また，この日本語版はTWSTRSを知らない第三者（上記とは別の科学技術翻訳専門の訳者および日本の神経内科医）によって再度英語に逆翻訳されたうえで，米国の専門家によって原著との表現や内容が異なっていないことを確認している。

2．評価尺度

TWSTRSは重症度，機能障害度および疼痛度を評価する3つの下位尺度から構成されるスケールである。このうち，TWSTRS-重症度スケールでは頸部の運動機能を評価するもので，Table 1に評価合計10項目を示した。TWSTRS-重症度スケールはA．最大偏倚，B．偏倚持続，C．感覚トリックの効果，D．肩挙上または肩の前方偏倚，E．自動運動域，F．頭位を正常に持続できる時間の評価項目，合計10項目（A．最大偏倚のみ5項目）で構成され，最大スコアは35点となる。また，Table 2にTWSTRS-重症度スケール[7]の評価項目を示した。

3．評価方法

2002年7月13日および2003年1月15日の2回に分けて，TWSTRS評価者間信頼性検討会を実施した。この検討会には異なる施設の神経内科医合計27名が参加した。この27名は3グループ（グループ1；10名，グループ2；10名，グループ3；7名）より構成されている。

評価者はまず，トレーニング用映像およびエラン社が米国でトレーニングを実施した際に使用したトレーニング用マニュアルを用い，評価項目に関して評価者間の評価基準の標準化を行った。その後に，患者映像例を見ながらTWSTRS-重症度スケールスコア記録用紙に評価を記載した。患者映像は1人分が15分間で，画像を見ながらA～Fを評価した。ビデオ画像はAから順番にFま

Table 2 TWSTRS -severity Scale

A．最大偏倚（異常運動に抵抗しない状態における最大偏倚運動を評価する。検者は患者の注意をそらすような，あるいは症状を増強させるような手段を用いてもよい。偏倚角度が2つのスコアの中間にある場合には，高スコアのほうを選ぶ。）

1．回旋（右旋，左旋）
- 0：なし
- 1：ごく軽度（可動域の1/4未満；1～22°）
- 2：軽度　（可動域の1/4～1/2；23～45°）
- 3：中等度　（可動域の1/2～3/4；46～67°）
- 4：高度　（可動域の3/4より大）；68～90°）

2．側屈（右屈，左屈；肩挙上は除外）
- 0：なし
- 1：軽度　（1～15°）
- 2：中等度（16～35°）
- 3：高度　（36°より大）

3．a）前屈（aまたはbの一方を評価）
- 0：なし
- 1：軽度の下顎偏倚
- 2：中等度の下顎偏倚（可動域の約1/2）
- 3：高度の下顎偏倚（下顎が胸に付くか，これに準じる）

3．b）後屈（aまたはbの一方を評価）
- 0：なし
- 1：軽度　（頭頂は後方を，下顎は上方へ偏倚）
- 2：中等度（可動域の約1/2）
- 3：高度　（可動域の限界に近い偏倚）

4．側方偏倚（右方，左方）
- 0：なし
- 1：あり

5．前後偏倚（前方，後方）
- 0：なし
- 1：あり

B．偏倚持続（最大偏倚〔患者に指示して最大偏倚を取らせた際の所見は除外する〕を評価した後，標準的な検査の過程における総括的なスコアを決定する。合計スコア算出の際には，本項目のスコアを2倍する。）

出現頻度（持続性）	最大偏倚を呈する割合
0：なし	
1：検査時間の25%未満	最大偏倚となることは少ないが，偏倚は持続する
2：検査時間の25%未満	最大偏倚が持続することが多い
検査時間の25～50%	最大偏倚となることは少ないが，偏倚は持続する
3：検査時間の25～50%	最大偏倚が持続することが多い
検査時間の50～75%	最大偏倚となることは少ないが，偏倚は持続する
4：検査時間の50～75%	最大偏倚が持続することが多い
検査時間の75%より大	最大偏倚となることは少ないが，偏倚は持続する
5：検査時間の75%より大	最大偏倚が持続することが多い

C．感覚トリックの効果
- 0：一種以上のトリックによって症状が完全に消失する
- 1：トリックによって症状が軽快する
- 2：トリックの影響は（ほとんど）ない

D．肩挙上または肩の前方偏倚
- 0：なし
- 1：軽度　（可動域の1/3未満）
- 2：中等度（可動域の1/3～2/3）で持続的〔観察時間の75%より大〕または重度（可動域の2/3より大）で間欠性
- 3：高度で持続性

E．自動運動域（多方向の運動制限を有する場合には，制限が最も強い方向で評価する）
- 0：偏倚の反対方向へ完全に動かせる
- 1：正中線を越えるが，可動域制限がある
- 2：正中線を越えることが困難
- 3：正中線に達しない
- 4：偏倚姿勢で（ほぼ）固定

F．頭位を正常に持続できる時間（60秒以内，2回の平均をとる）
- 0：60秒より大
- 1：46～60秒
- 2：31～45秒
- 3：16～30秒
- 4：15秒より小

＊ Quoted from refarence[7]

でを評価する構成ではなく，画像が流れる15分間全体ですべての項目を評価した。また，Bの「偏倚の持続」に関しては，映像が流れている全時間から，Cの「感覚トリック」，Eの「自動運動域」およびFの「頭位を正常に維持できる時間」の時間を除いて評価した。

グループごとに2名の患者映像例を約5分の間隔をあけて順番に評価した。なお，評価順序による評価の偏りを防止するため，グループ1とグループ3は患者映像1，

Table 3 Scores and summary statistics of TWSTRS-severity Scale (patient 1)

	A						B	C	D	E	F	Total
	A 1	A 2	A 3	A 4	A 5	Total of A 0-12	0-10	0-2	0-3	0-4	0-4	0-35
Numbers of rater	27	27	27	27	27	27	27	27	27	27	27	27
Mean	0.9	0.7	1.6	0.4	0.9	4.5	7.6	1.1	1.1	0.6	2.9	17.8
Standard deviation	0.6	0.5	0.5	0.5	0.3	1.3	1.2	0.3	0.5	0.5	0.9	2.0
Maximum	2	2	2	1	1	7	10	2	2	1	4	21
Minimum	0	0	1	0	0	3	6	1	0	0	0	12
Reference (Mean of 3 raters)	1	1	2	0	1	5	8	1	1	1	3	18

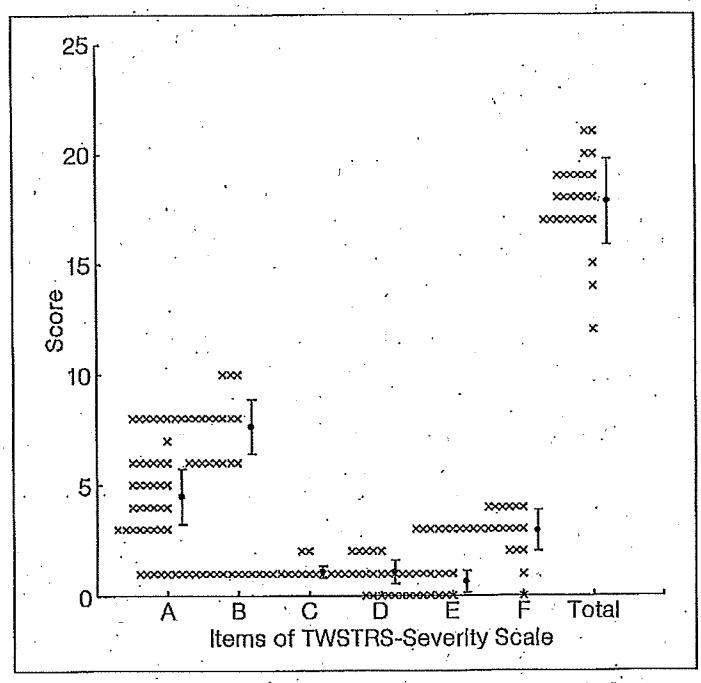

Fig. 1 Scores of each rater and summary statistics of the TWSTRS-severity Scale (patient 1)

患者映像2の順に評価し，グループ2は患者映像2，患者映像1の順に評価した。なお，2002年7月13日にはグループ1とグループ2が，2003年1月15日にはグループ3が検討会に参加した。

評価者はグループ別に遮蔽された場所で評価を行った。さらにグループ内の評価者はそれぞれ独立して評価していることを確認した。試験の管理者はビデオ終了後，すべての評価者が評価を終えたことを確認し，記載不備あるいは記載内容が不明瞭な箇所がないことを評価者とともに確認したうえで，スコア記録用紙を回収した。

4．解析方法

解析はエーザイ株式会社において，統計解析ソフトSAS for windows (release 6.12以上) を用いて実施した。解析は記述統計を用いた推定を中心にして行った。

解析項目に対して，Fleissの級内相関係数(Intraclass Correlation Coefficient: ICC)[8]を算出した。さらに，級内相関係数の95%信頼区間の下限を算出した。

II. 結　　果

1．解析対象集団

信頼性試験に参加した評価者は合計で27名であり，それらの評価者によりTWSTRS-重症度スケールは2映像とも全項目が判定された。これら2映像分の全評価項目を解析に用いた。